DEC 1 1967

OAK RIDGE NATIONAL LABORATORY
operated by
UNION CARBIDE CORPORATION
NUCLEAR DIVISION
for the
U.S. ATOMIC ENERGY COMMISSION

UNION CARBIDE

ORNL-TM-1997

MASTER

AN EVALUATION OF THE MOLTEN SALT REACTOR EXPERIMENT HASTELLOY N SURVEILLANCE SPECIMENS – FIRST GROUP

H. E. McCoy, Jr.

ORNL-TM-1997

Contract No. W-7405-eng-26

METALS AND CERAMICS DIVISION

AN EVALUATION OF THE MOLTEN SALT REACTOR EXPERIMENT HASTELLOY N SURVEILLANCE SPECIMENS — FIRST GROUP

H. E. McCoy, Jr.

NOVEMBER 1967

OAK RIDGE NATIONAL LABORATORY
Oak Ridge, Tennessee
operated by
UNION CARBIDE CORPORATION
for the
U.S. ATOMIC ENERGY COMMISSION

CONTENTS

AN EVALUATION OF THE MOLTEN SALT REACTOR EXPERIMENT HASTELLOY N SURVEILLANCE SPECIMENS — FIRST GROUP

H. E. McCoy, Jr.

ABSTRACT

We have tested the first group of surveillance specimens from the Molten Salt Reactor Experiment core. They were removed after 7823 Mwhr of reactor operation during which the specimens were held at 645 ± 10°C for 4800 hr and accumulated a thermal dose of 1.3×10^{20} neutrons/cm^2. The high-temperature ductility was reduced, but the reduction was similar to that observed for these materials when irradiated in the Oak Ridge Reactor in a helium environment. The low-temperature ductility was reduced, and this is thought to be due to the formation of intergranular M_6C. The specimens showed no evidence of corrosion; however, a carbon-rich layer, 1 to 2 mils in depth, was noted where the Hastelloy N and graphite were in contact. The mechanical properties of the Hastelloy N appear adequate for the continued satisfactory operation of the MSRE.

Test results are presented for the effects of several variables on the tensile ductility of irradiated and unirradiated Hastelloy N. These variables included test temperature, strain rate, and prestraining.

INTRODUCTION

The Molten Salt Reactor Experiment is a single region reactor that is fueled by a molten fluoride salt (65 LiF, 29.1 BeF_2, 5 ZrF_4, 0.9 UF_4 mole %), moderated by unclad graphite, and contained by Hastelloy N (Ni–16 Mo–7 Cr–4 Fe–0.05 C, wt %). The details of the reactor design and construction can be found elsewhere.[1] We knew that the neutron environment would produce some changes in the two structural materials — graphite and Hastelloy N. Although we were very confident of the compatibility of these

---

[1]R. C. Robertson, MSRE Design and Operations Report, Pt. 1, Description of Reactor Design, ORNL-TM-728 (January 1965).

materials with the fluoride salt, we needed to keep abreast of the possible development of corrosion problems within the reactor itself. For these reasons, we developed a surveillance program that would allow us to follow the property changes of graphite and Hastelloy N specimens as the reactor operated.

The reactor went critical on June 1, 1965, and after numerous small problems were solved, assumed normal operation on May 1966. The present group of surveillance specimens was in the reactor from September 8, 1965, to July 28, 1966, and was removed after 7823 Mwhr of operation (designated "first group"). This report covers the tests that were run on the Hastelloy N specimens that were removed.

EXPERIMENTAL DETAILS

Surveillance Assembly

The core surveillance assembly was designed by W. H. Cook and others, and the details have been reported previously.[2] The facility is shown pictorially and schematically in Fig. 1. The specimens are arranged in three stringers. Each stringer is about 62 in. long and consists of two Hastelloy N rods and a graphite section made up of various pieces that are joined by pinning and tongue-and-groove joints. The Hastelloy N rod has periodic reduced sections 1 1/8 in. long × 1/8 in. in diameter and can be cut into small tensile specimens after it is removed from the reactor. Three stringers are joined together so that they can be separated in a hot cell and reassembled with one or more new stringers for reinsertion into the reactor. The assembled stringers fit into a perforated Hastelloy N basket that is inserted into an axial position about 3.6 in. from the core center line.

[2]W. H. Cook, MSR Program Semiann. Progr. Rept. Aug. 31, 1965, ORNL-3872, p. 87.

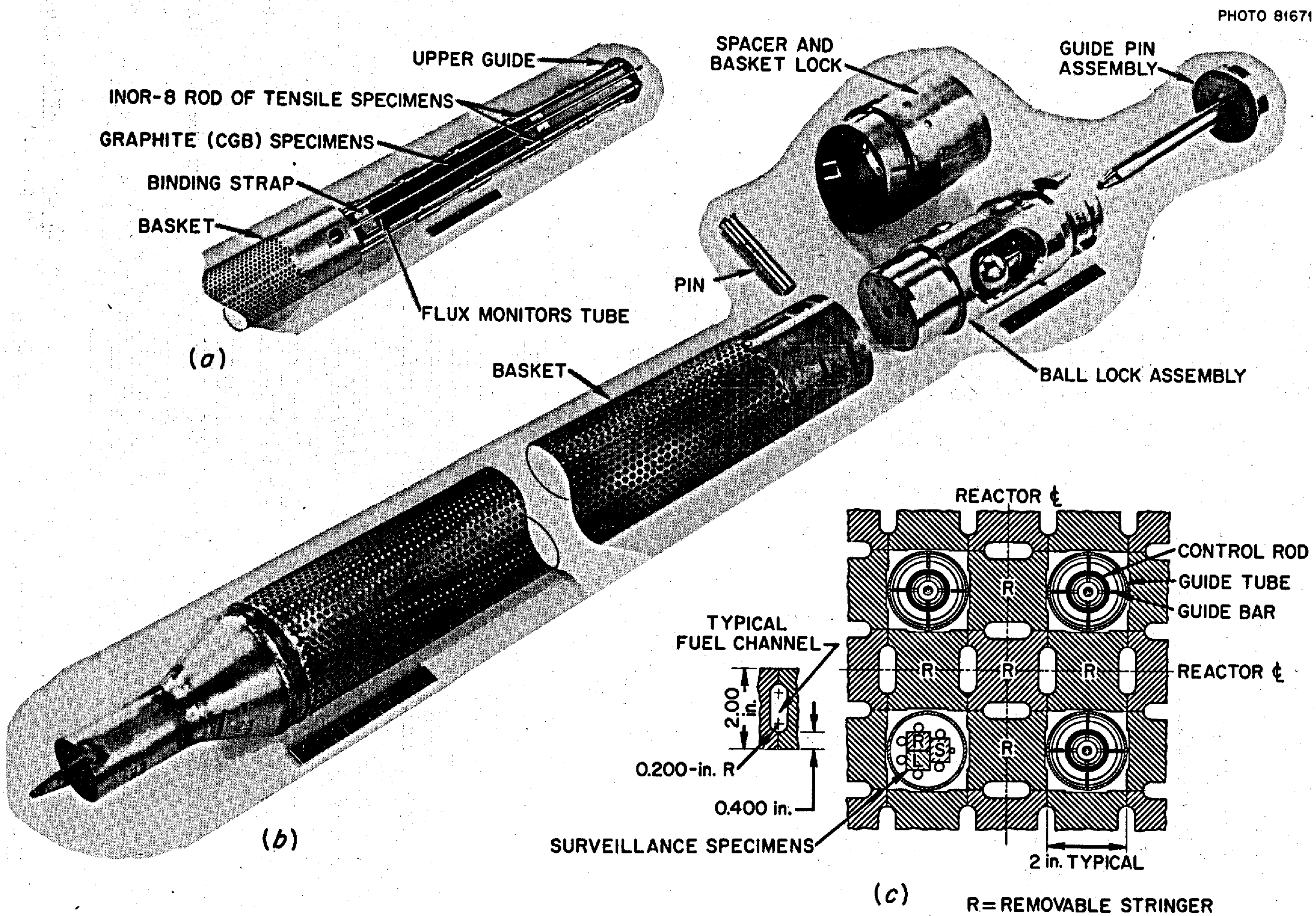

Fig. 1. MSRE Surveillance Fixture.

When the basket was removed on July 28, 1966, some of the specimens were bent and the entire assembly had to be replaced.[3] Slight modifications in the design were made, and the assembly was removed recently and found to be in excellent condition.[4]

A control facility is associated with the surveillance program. It utilizes a "fuel salt" containing depleted uranium in a static pot that is heated electrically. The temperature is controlled by the MSRE computer so that the temperature matches that of the reactor. Thus, these specimens are exposed to conditions the same as those in the reactor except for the static salt and the absence of a neutron flux.

There is another surveillance facility for Hastelloy N located outside the core in a vertical position about 4.5 in. from the vessel. These specimens are exposed to the cell environment (N_2 + 2–5% O_2). They were not removed during the first group.

Materials

Two heats of Hastelloy N were used in this program: heats 5081 and 5085. Both of these heats were air-melted by Stellite Division of Union Carbide Corporation, and their chemical analyses are given in Table 1. Heat 5085 was used for making the cylindrical portion of the core vessel, and heat 5081 was used for various parts inside the reactor.

Test Specimens

The specimens were put into the reactor as rods 62 in. long by 1/4 in. in diameter with reduced sections 1/8 in. in diameter by 1 1/8 in. long. The long rod was made in seven pieces and welded together to obtain the 62-in.-long rod. After removal from the reactor, the rod was sawed into small specimens with a gage section 1 1/8 in. long by 1/8 in. in diameter. Each rod is designated by a letter and the individual

---

[3]W. H. Cook, MSR Program Semiann. Progr. Rept. Aug. 31, 1966, ORNL-4037, p. 97.

[4]W. H. Cook, "Molten Salt Reactor Program," Metals and Ceramics Div. Ann. Progr. Rept. June 30, 1967, ORNL-4170, Chap. 34 (in press).

Table 1. Chemical Analysis of Surveillance Heats

Element	Content, wt %	
	Heat 5085	Heat 5081
Cr	6.2	6.1
Fe	3.3	3.4
Mo	16.3	16.4
C	0.054	0.059
Si	0.58	0.52
Co	0.15	0.10
W	0.07	0.07
Mn	0.67	0.65
V	0.20	0.20
P	0.013	0.012
S	0.004	0.002
Al	0.02	0.05
Ti	<0.01	<0.01
Cu	0.01	0.01
B	0.0038	0.0050
Ni	bal	bal

specimens are numbered beginning at the bottom of the rod and increasing to 27 at the top.

The rods in the first group were bent, and it was necessary to examine each specimen with an optical comparator to determine whether it was suitable for use. If the total indicated runout of the gage section was greater than 0.002 in., the specimen was not used. The best specimens were used for the higher temperature tests where the expected strains were smallest. The results from a brittle material are affected more seriously by specimen alignment than are those from a ductile material.

The materials were received in the mill annealed condition (1 hr at 1177°C). They were given a further anneal of 2 hr at 900°C prior to insertion into the reactor and the control facility.

Irradiation Conditions

The specimens from the first group were in the reactor from September 8, 1965, to July 28, 1966. The reactor had operated 0.0066 Mwhr when the specimens were inserted and 7823 Mwhr when they were removed. They were at temperature for 4800 hr with the temperature range being 645 ± 10°C. However, the material was only exposed to salt for 2796 hr. The flux was measured by H. B. Piper[5] using stainless steel wires that were attached to the surveillance specimens. The thermal and fast flux profiles are shown in Figs. 2 and 3 along with the axial location of each specimen. The peak thermal dose, based on the $^{59}Co(n,\gamma)^{60}Co$ transmutation, was 1.3×10^{20} neutrons/cm^2 and the fast dose (>1.22 Mev), based on the $^{58}Ni(n,p)^{58}Co$ transmutation, was 3×10^{19} neutrons/cm^2. The cross section used for the $^{59}Co(n,\gamma)^{60}Co$ transmutation was 22.25 barns, and that for the $^{58}Ni(n,p)^{58}Co$ transmutation was 0.1262 barns.

---

[5]H. B. Piper, private communication.

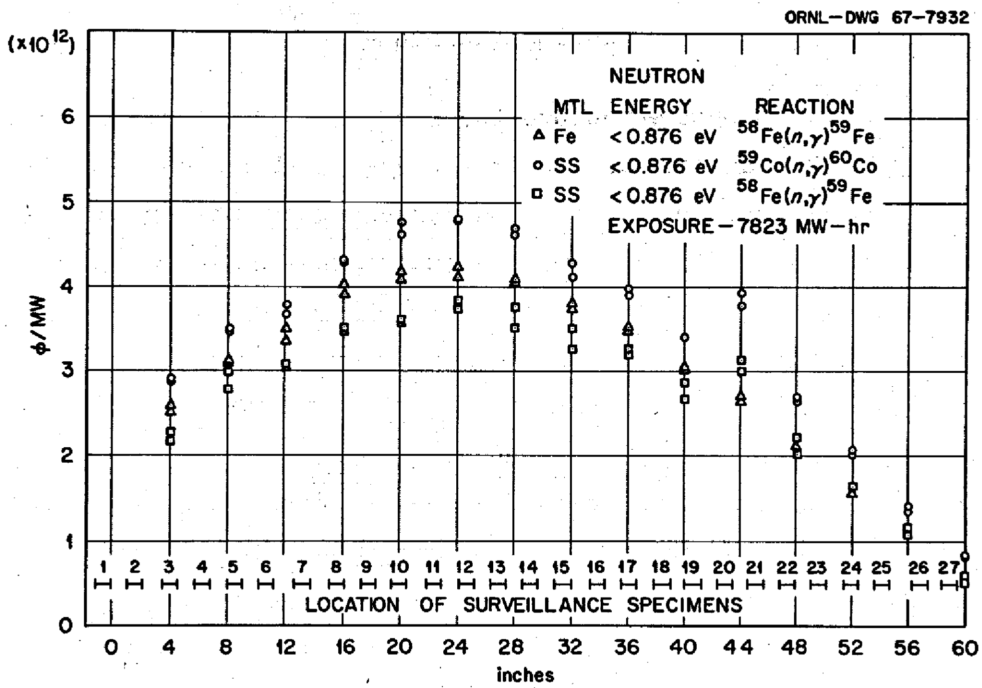

Fig. 2. Measurements of the Thermal Flux for the MSRE Core Specimens — First Group.

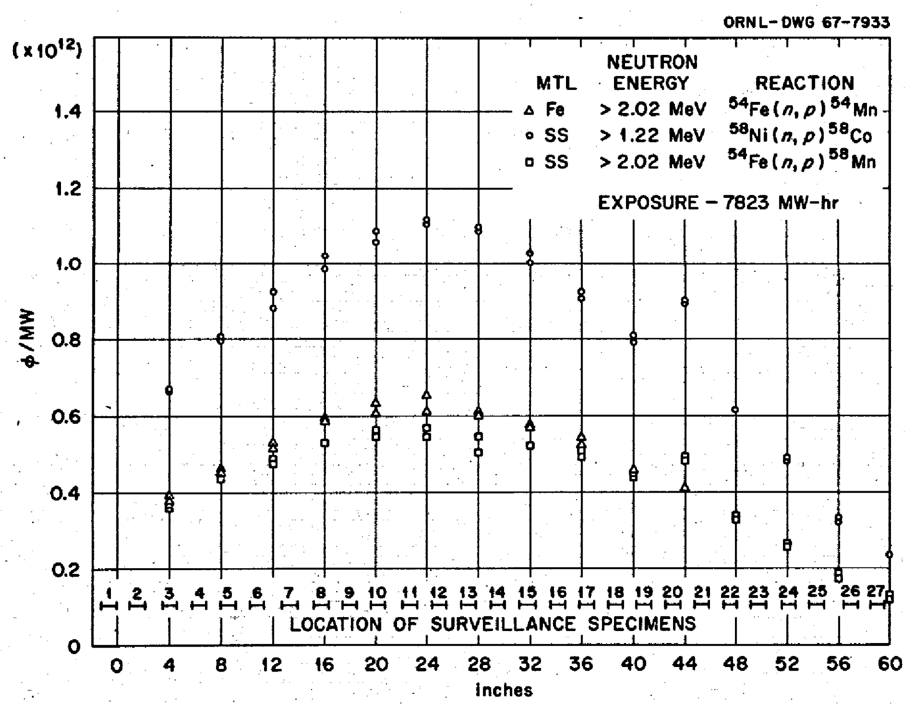

Fig. 3. Measurements of the Fast Flux for the MSRE Core Specimens — First Group.

Testing Techniques

The laboratory creep-rupture tests were run in conventional creep machines of the dead load and lever arm types. The strain was measured by a dial indicator that showed the total movement of the specimen and part of the load train. The zero strain measurement was taken immediately after the load was applied. The temperature accuracy was ±0.75%, the guaranteed accuracy of the Chromel-P—Alumel thermocouples used.

The postirradiation creep-rupture tests were run in lever arm machines that were located in hot cells. The strain was measured by an extensometer with rods attached to the upper and lower specimen grips. The relative movement of these two rods was measured by a linear differential transformer, and the transformer signal was recorded. The accuracy of the strain measurements is difficult to determine. The extensometer (mechanical and electrical portions) produced measurements that could be read to about ±0.02% strain; however, other factors (temperature changes in the cell, mechanical vibrations, etc.) probably combined to give an overall accuracy of ±0.1% strain. This is considerably better than the specimen-to-specimen reproducibility that one would expect for relatively brittle materials. The temperature measuring and control system was the same as that used in the laboratory with only one exception. In the laboratory, the control system was stabilized at the desired temperature by use of a recorder with an expanded scale. In the tests in the hot cells, the control point was established by setting the controller without the aid of the expanded-scale recorder. This error and the thermocouple accuracy combine to give a temperature uncertainty of about ±1%.

The tensile tests were run on Instron Universal Testing Machines. The strain measurements were taken from the crosshead travel.

The test environment was air in all cases. Metallographic examination showed that the depth of oxidation was small (<0.002 in.), and hence we feel that the environment did not appreciably influence the test results.

Test Results

Since the surveillance assembly was bent, it was necessary to remove all the specimens in the first group, and we had about 50 specimens of each heat after the bent ones were discarded. Thus, we had enough specimens to run the desired tests for surveillance purposes and enough to look at some further variables that are of value in understanding the behavior of irradiated Hastelloy N. We shall present all the results that were obtained even though much of this information has little direct bearing on the safe operation of the MSRE. Since the rupture ductility is of primary importance, we shall be most concerned with this property.

The results of tensile tests on the control specimens of heat 5081 are given in Table 2. The total elongations at fracture as a function of temperature are shown in Fig. 4 for strain rates of 0.05 and 0.002 min^{-1}. This material exhibits the ductility minimum that is characteristic of nickel-base alloys. The temperature of the minimum ductility seems to decrease with decreasing strain rate. Several of the specimens were run at various strain rates over the range of 2 to 0.002 min^{-1}. The results of these tests are also given in Table 2, and the fracture elongations are given in Fig. 5. The fracture elongation is very sensitive to strain rate at 650°C, but relatively insensitive at higher and lower temperatures.

The results of the tests on the surveillance specimens from heat 5081 are summarized in Table 3. The elongation at fracture is plotted as a function of temperature in Fig. 6. The irradiated material is characterized by a sharp drop in ductility with increasing temperature above about 500°C. The ductility continues to decrease with increasing temperature rather than exhibiting a ductility minimum like the unirradiated material (Fig. 4). The ductility is lower at a strain rate of 0.002 min^{-1} than at 0.05 min^{-1}, but the difference decreases with increasing temperature. This point is demonstrated quite well in Fig. 7 where the dependence of the ductility on strain rate is shown for several temperatures.

We have looked individually at the properties of the surveillance and control specimens of heat 5081; let us now compare these properties. The ratios of the property for the irradiated material to that of the unirradiated material are compared in Fig. 8 as a function of temperature.

Table 2. Results of Tensile Tests on MSRE Surveillance Control Specimens Heat 5081

Specimen Number	Test Temperature (°C)	Strain Rate (min^{-1})	Stress (psi) Yield	Stress (psi) Ultimate	Elongation (%) Uniform	Elongation (%) Total	Reduction in Area (%)	True Fracture Strain (%)
AC-8	25	0.05	47,700	118,700	55.9	57.6	48.8	67.4
AC-11	200	0.05	40,200	107,100	53.3	54.6	42.0	58.9
CC-27	400	2	41,400	94,500	50.4	53.6	42.4	55.7
CC-26	400	0.5	34,600	97,000	53.7	58.2	46.6	63.1
CC-25	400	0.2	36,300	97,900	52.2	53.8	42.7	56.0
AC-22	400	0.05	36,700	100,600	51.0	52.0	48.7	66.8
CC-24	400	0.02	37,800	99,900	51.7	56.0	41.7	54.4
CC-23	400	0.005	34,700	97,400	55.4	56.3	44.0	58.6
BC-8	400	0.002	37,100		52.9	55.2	46.7	63.0
CC-21	500	2	36,200	93,200	52.0	56.0	48.8	67.4
CC-19	500	2	35,200	92,700	52.4	56.0	42.6	55.8
CC-29	500	0.5	52,600	105,400	45.8	49.4	40.5	52.0
CC-18	500	0.2	36,800	98,800	55.0	57.0	51.1	72.0
AC-19	500	0.05	35,800	97,800	53.6	56.6	46.2	62.0
CC-17	500	0.02	34,900	97,600	55.5	56.6	46.2	62.5
CC-16	500	0.005	34,700	92,500	54.4	55.4	40.3	51.6
AC-24	500	0.002	35,000	97,700	44.9	45.3	33.6	41.0
BC-9	500	0.002	36,200	95,300	46.2	47.0	38.1	48.2
AC-20	550	0.05	35,900	93,300	49.7	51.1	40.3	51.8
AC-25	550	0.002	37,300	80,300	22.8	23.7	23.0	26.2
AC-18	600	0.05	34,900	81,200	31.8	32.3	31.0	37.2
AC-29	600	0.002	37,400	71,400	21.3	21.7	19.9	22.4

Table 2 (continued)

Specimen Number	Test Temperature (%)	Strain Rate (min^{-1})	Stress (psi) Yield	Stress (psi) Ultimate	Elongation (%) Uniform	Elongation (%) Total	Reduction in Area (%)	True Fracture Strain (%)
BC-10	650	2	36,300	88,500	51.5	52.4	36.9	46.3
CC-8	650	2	42,400	85,200	44.4	46.8	37.2	46.5
AC-4	650	0.5	32,900	81,500	37.1	39.0	28.8	34.0
AC-10	650	0.2	36,300	78,200	28.5	29.3	23.4	26.4
AC-27	650	0.05	32,400	68,400	23.8	24.6	23.1	26.2
AC-7	650	0.02	34,400	65,200	16.8	17.7	19.0	21.1
AC-5	650	0.005	33,900	68,400	22.6	23.1	24.4	28.0
AC-17	650	0.002	33,600	66,700	22.8	23.2	21.6	21.4
AC-28	700	0.05	39,500	68,400	18.8	19.8	25.8	14.9
AC-16	700	0.002	32,400	63,100	20.0	29.3	23.5	21.7
CC-2	760	2	41,600	76,600	36.8	40.8	24.4	28.0
CC-9	760	0.5	30,800	72,700	37.1	40.2	30.7	36.9
CC-5	760	0.2	32,100	71,900	33.3	38.9	21.9	24.7
AC-12	760	0.05	29,900	64,500	25.1	41.6	35.0	43.1
CC-4	760	0.02	32,400	63,800	20.0	43.8	42.4	55.3
CC-3	760	0.005	32,700	54,500	12.7	39.2	41.0	52.9
AC-14	760	0.002	32,600	47,200	9.4	39.5	42.7	56.0
CC-15	850	2	33,200	66,300	30.0	48.0	46.3	62.5
CC-14	850	0.5	28,900	60,600	23.2	49.2	43.9	58.2
CC-12	850	0.2	29,600	54,100	16.3	51.4	50.8	71.1
AC-6	850	0.05	28,300	43,400	11.2	53.2	49.8	69.0
CC-11	850	0.02	30,000	40,400	7.8	43.6	48.7	67.0
CC-10	850	0.005	29,200	30,600	2.0	44.4	50.9	71.6
AC-15	850	0.002	26,400	26,400	1.5	45.0	43.9	58.3

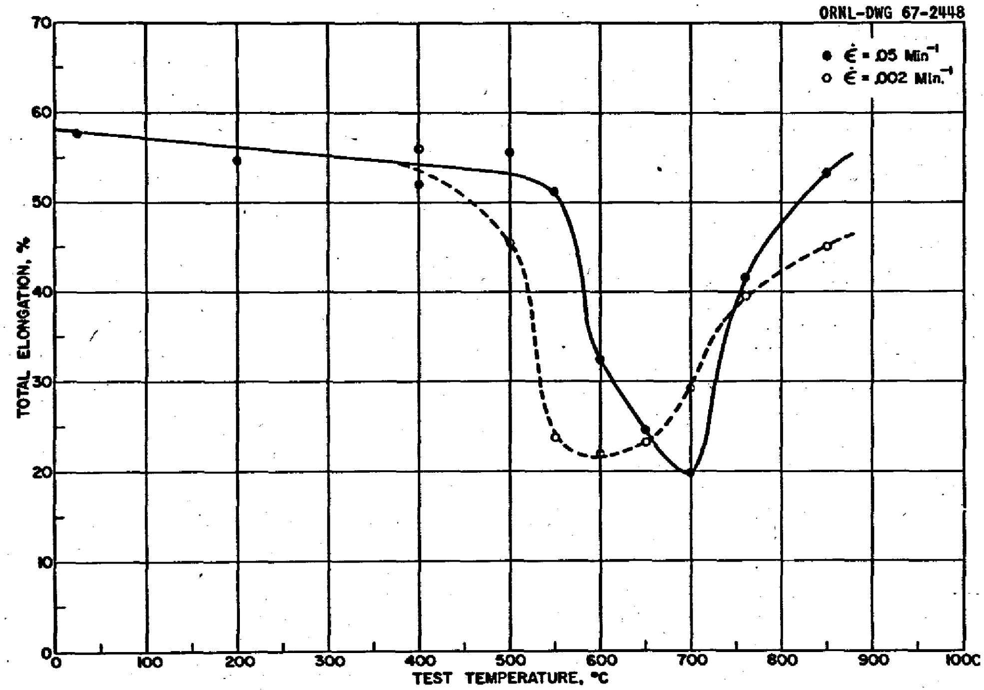

Fig. 4. Tensile Ductilities of MSRE Surveillance Control Specimens, Heat 5081.

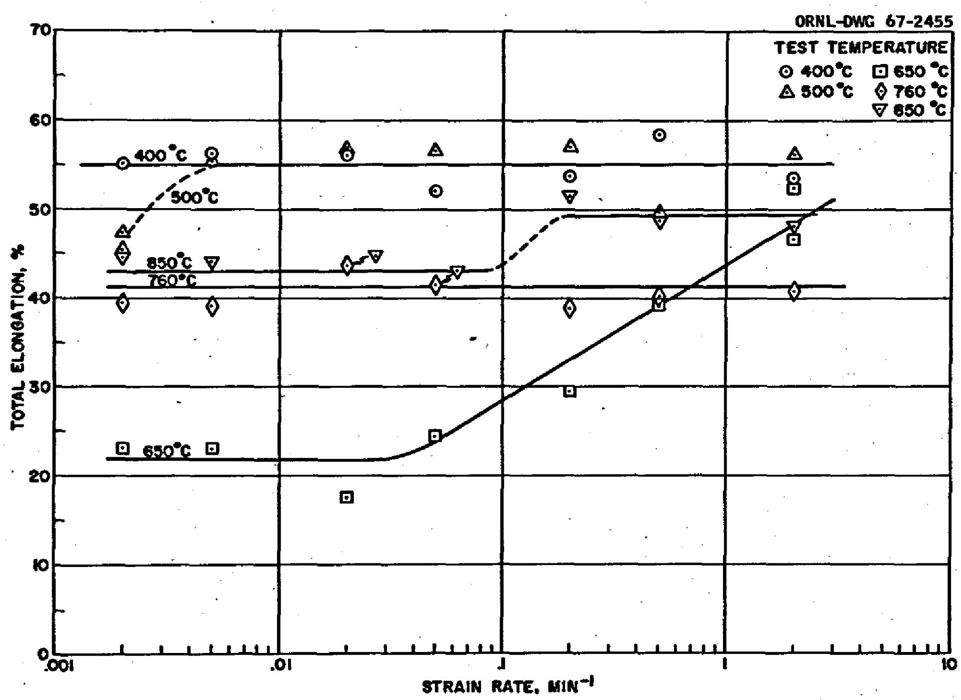

Fig. 5. Influence of Strain Rate on the Ductility of MSRE Surveillance Control Specimens, Heat 5081.

Table 3. Results of Tensile Tests on MSRE Surveillance Specimens
Heat 5081

Specimen Number	Test Temperature (°C)	Strain Rate (min^{-1})	Stress (psi)		Elongation (%)		Reduction in Area (%)	True Fracture Strain (%)
			Yield	Ultimate	Uniform	Total		
D-16	25	0.05	51,100	105,500	38.5	38.7	31.3	37.0
D-19	25	0.05	54,100	109,000	42.6	42.6	25.9	30.0
D-15	200	0.05	42,700	99,600	49.0	49.4	33.3	40.7
F-2	400	2	41,200	91,400	49.2	51.6	34.4	42.0
F-1	400	0.5	43,700	88,300	33.2	33.9	32.5	39.5
E-15	400	0.5	39,900	93,800	48.3	49.1	33.9	41.5
F-7	400	0.2	38,300	92,200	49.4	51.0	37.2	46.9
D-24	400	0.05	37,100	94,100	49.3	50.9	33.3	40.7
F-23	400	0.02	37,800	91,700	45.8	46.1	36.0	44.7
F-10	400	0.005	38,800	93,300	49.9	50.4	37.7	47.7
F-19	400	0.002	39,100	92,500	47.1	47.7	32.3	38.9
F-5	450	0.002	38,200	86,900	37.8	38.6	25.8	30.1
F-8	500	2	44,000	85,600	44.4	46.0	31.6	38.2
F-20	500	0.5	36,400	87,000	43.1	44.1	36.2	45.2
E-6	500	0.2	37,300	86,500	47.8	48.5	32.1	38.7
D-9	500	0.05	38,600	90,200	50.6	51.0	31.9	38.7
E-25	500	0.02	36,600	83,600	37.0	37.5	30.2	35.8
E-12	500	0.005	38,000	76,800	23.3	24.1	24.2	27.8
F-13	500	0.002	38,800	75,800	22.4	23.1	21.9	24.9
E-9	500	0.002	38,000	84,800	31.0	32.1	29.8	35.4
D-25	550	0.05	35,400	77,800	31.6	32.1	26.1	30.3
F-27	550	0.002	42,200	62,700	11.8	13.8	3.34	6.5
E-23	600	0.05	35,200	74,800	25.6	26.4	31.8	38.2
E-24	600	0.002	36,100	62,100	15.0	15.8	16.7	18.3

Table 3 (continued)

Specimen Number	Test Temperature (°C)	Strain Rate (min^{-1})	Stress (psi) Yield	Stress (psi) Ultimate	Elongation (%) Uniform	Elongation (%) Total	Reduction in Area (%)	True Fracture Strain (%)
F-18	650	2	36,700	61,100	20.8	24.0	21.8	24.4
F-6	650	0.5	33,400	63,900	18.2	18.9	15.4	16.9
F-26	650	0.5	30,500	34,900	2.6	3.7	2.9	21.5
F-3	650	0.5	34,300	75,600	34.0	35.3	29.1	58.4
E-3	650	0.2	37,200	64,200	14.9	15.8	22.5	25.4
E-7	650	0.05	34,600	57,200	13.8	14.3	13.9	14.8
E-13	650	0.02	33,800	53,600	11.1	12.9	17.6	19.1
E-19	650	0.005	34,600	53,000	10.8	11.3	14.6	15.9
E-14	650	0.002	34,400	48,400	8.2	9.0	11.6	12.2
E-22	700	0.05	31,700	53,900	13.8	14.2	12.9	13.9
E-2	700	0.002	33,800	44,000	4.8	5.5	6.7	6.9
F-22	760	2	36,100	57,600	18.8	22.0	14.7	15.9
D-8	760	0.5	31,000	49,100	12.0	12.9	11.0	11.5
D-13	760	0.2	31,300	49,400	11.9	12.4	10.2	10.5
E-8	760	0.05	31,400	43,200	6.7	7.4	6.2	6.1
D-10	760	0.02	32,000	42,200	5.2	5.7	4.6	4.6
D-27	760	0.005	36,500	40,600	4.0	4.3	2.6	2.6
E-20	760	0.002	32,100	36,700	1.9	3.9	3.5	3.6
E-4	850	2			4.4	8.4	8.7	9.0
E-27	850	0.5	32,700	39,100	3.5	4.6	5.4	5.5
E-1	850	0.2	33,600	38,600	3.0	3.8	1.6	0.8
F-17	850	0.05	30,700	32,400	1.8	2.3	2.3	2.4
D-14	850	0.02	30,600	30,700	1.2	2.0	1.7	0.9
D-23	850	0.005	20,200	20,200	0.7	2.0	0.3	0.2
E-21	850	0.002	21,800	21,800	0.7	2.1	0.7	0.3

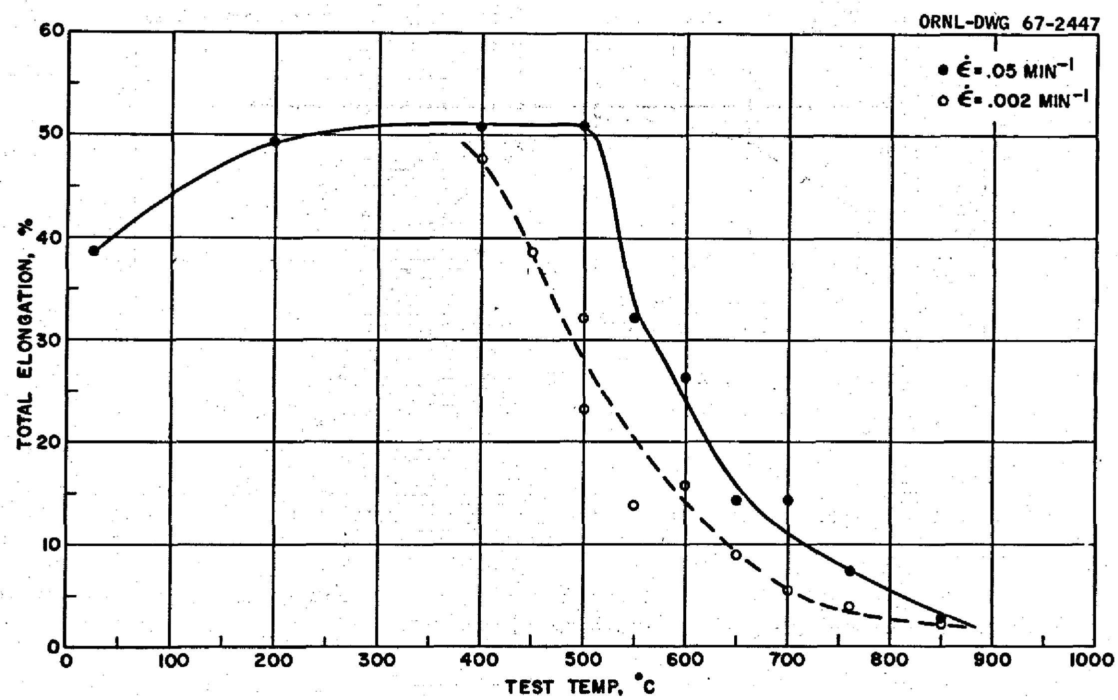

Fig. 6. Tensile Ductility of MSRE Surveillance Specimens, Heat 5081.

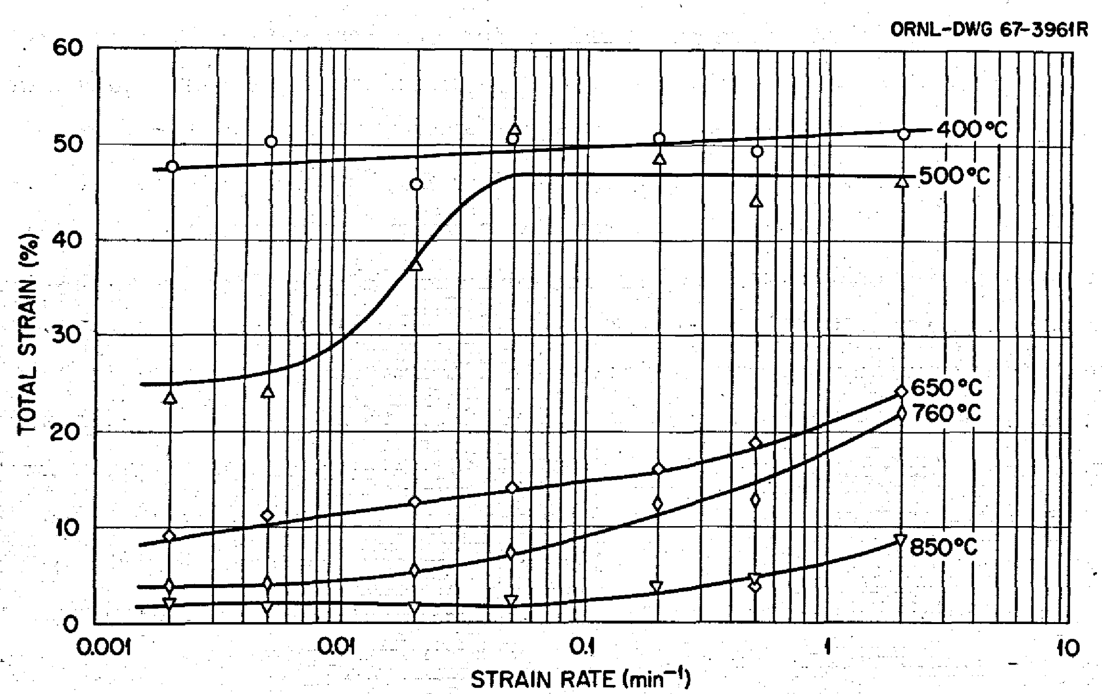

Fig. 7. Influence of Strain Rate on the Ductility of Hastelloy N (Heat 5081) — MSRE Surveillance Specimens.

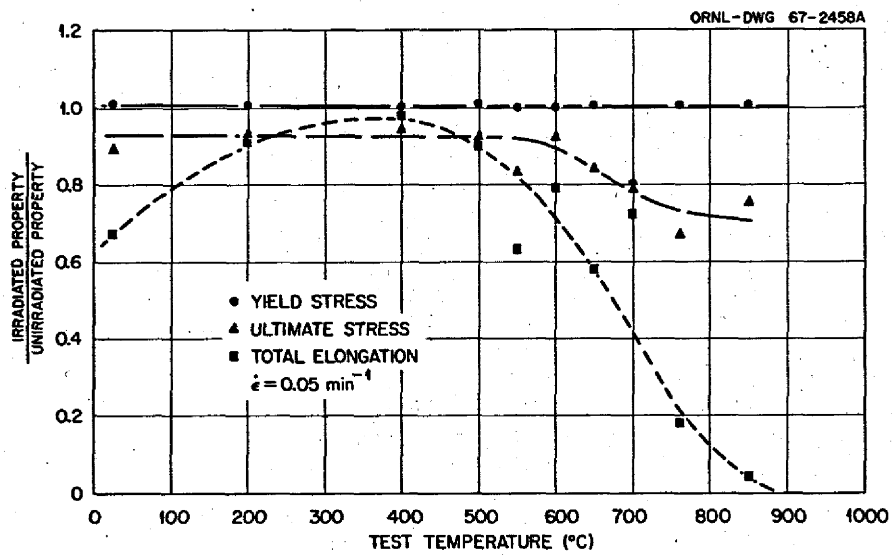

Fig. 8. Comparative Tensile Properties of Irradiated and Unirradiated MSRE Surveillance Specimens, Heat 5081.

The yield stress is unaffected by irradiation. The ultimate stress is reduced approximately 8% up to about 600°C where the reduction becomes greater with increasing temperature.

The total elongation at fracture for the irradiated material is lower by about 30% at room temperature, but recovers to be almost equivalent at 400°C. As the temperature is increased above 400°C, the ductility of the irradiated material drops to where it is only about 4% of that of the unirradiated specimens. The strain rate versus temperature data are treated in a similar way in Fig. 9. At 400°C the surveillance and control specimens have about the same ductility with only a slight decrease in the ratio with decreasing strain rate. At 500°C there is a sharp drop in the ratio at a strain rate of about 0.05 min^{-1}. This sharp change in strain rate sensitivity is probably due to the transition from transgranular to intergranular fracture. The ratio is a bit confusing at 650°C; its rise with decreasing strain rate is due to the fact that the ductility of the control specimens decreases more rapidly with decreasing strain rate than that of the surveillance specimens. At 760 and 850°C the ratio becomes quite small and its dependence on strain rate becomes less.

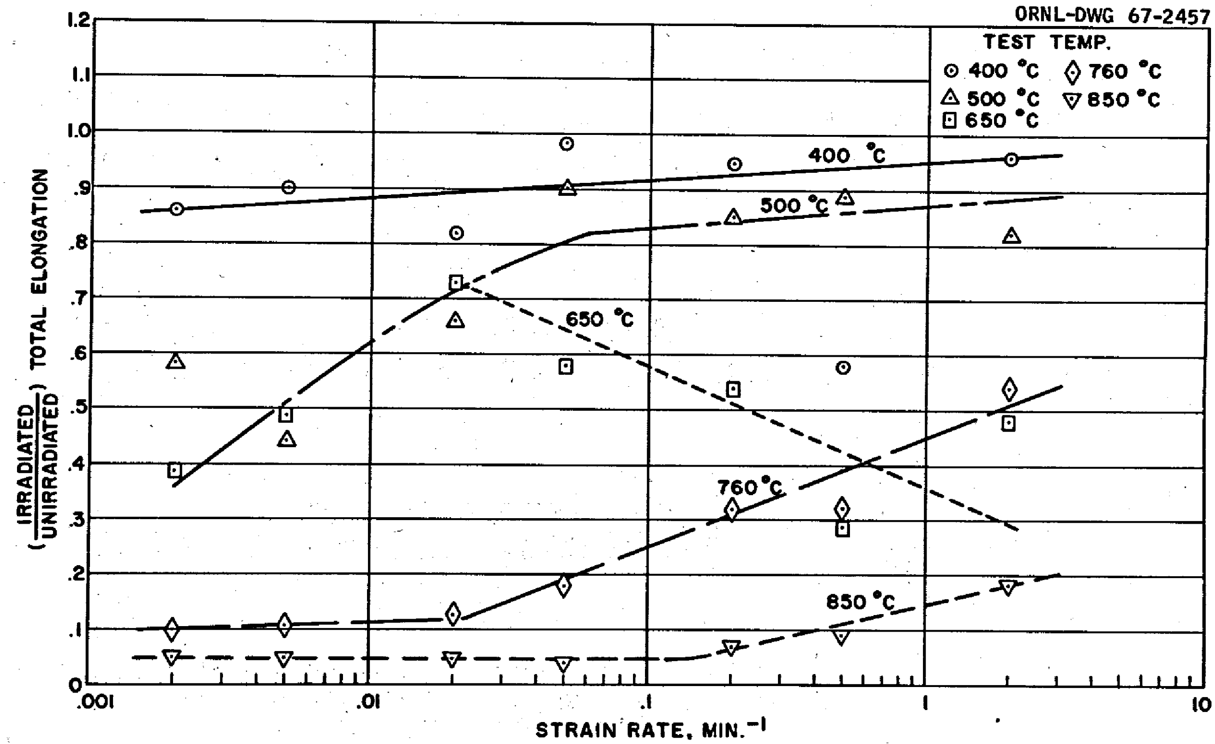

Fig. 9. Comparative Ductilities of MSRE Surveillance Specimens as a Function of Strain Rate, Heat 5081.

The results of the tensile tests on the control specimens of heat 5085 are given in Table 4. The total elongation at fracture is plotted in Fig. 10 as a function of the test temperature. The characteristic ductility minimum is obtained, but the temperature of the minimum ductility does not appear to be sensitive to strain rate.

The results of the tensile tests on the surveillance specimens from heat 5085 are given in Table 5. The fracture elongation is plotted as a function of test temperature in Fig. 11. The ductility drops precipitously above 500°C with the elongation being lower at the lower strain rate.

The ratio of the irradiated property to that of the unirradiated property for heat 5085 is shown in Fig. 12 as a function of temperature. The yield and ultimate stresses of this heat are influenced about the same by irradiation as those of heat 5081 (Fig. 8). The elongation at low temperatures is not reduced as much by irradiation, but it does not recover as the test temperature is increased.

Table 4. Results of Tensile Tests on MSRE Surveillance Control Specimens
Heat 5085

Specimen Number	Test Temperature (°C)	Strain Rate (min^{-1})	Stress (psi)		Elongation (%)		Reduction in Area (%)	True Fracture Strain (%)
			Yield	Ultimate	Uniform	Total		
DC-24	25	0.05	46,200	109,200	40.0	40.0	28.61	33.8
FC-3	25	0.05	45,500	111,200	46.8	46.8	31.45	39.5
DC-20	200	0.05	39,100	105,200	48.6	49.8	36.69	46.1
DC-23	400	0.05	34,800	95,800	47.6	48.8	39.01	49.6
DC-19	500	0.05	33,600	94,300	48.8	49.3	41.48	54.1
DC-26	500	0.002	33,400	91,700	43.3	44.3	37.78	47.7
DC-18	550	0.05	33,700	89,200	47.0	47.5	35.19	43.4
DC-13	550	0.002	32,500	74,000	26.5	27.5	26.1	30.2
FC-2	550	0.002	33,600	77,900	30.3	31.0	33.98	41.6
DC-17	600	0.05	32,200	78,300	33.8	34.6	32.60	37.8
DC-16	600	0.002	32,100	69,600	26.5	27.3	25.55	29.6
DC-14	650	0.05	31,800	70,100	25.8	26.8	29.97	35.9
DC-25	650	0.002	31,500	62,500	22.8	24.3	27.15	31.8
DC-5	700	0.05	29,200	64,000	28.4	29.5	28.14	33.2
DC-10	700	0.002	30,900	62,100	22.3	28.3	24.04	27.5
DC-3	760	0.05	28,100	60,800	27.0	33.0	32.16	38.7
DC-9	760	0.002	28,900	51,500	11.0	35.1	36.07	44.8
DC-22	850	0.05	25,700	45,100	11.5	38.8	47.23	64.1
DC-8	850	0.002	27,900	28,400	1.4	39.2	43.76	55.7

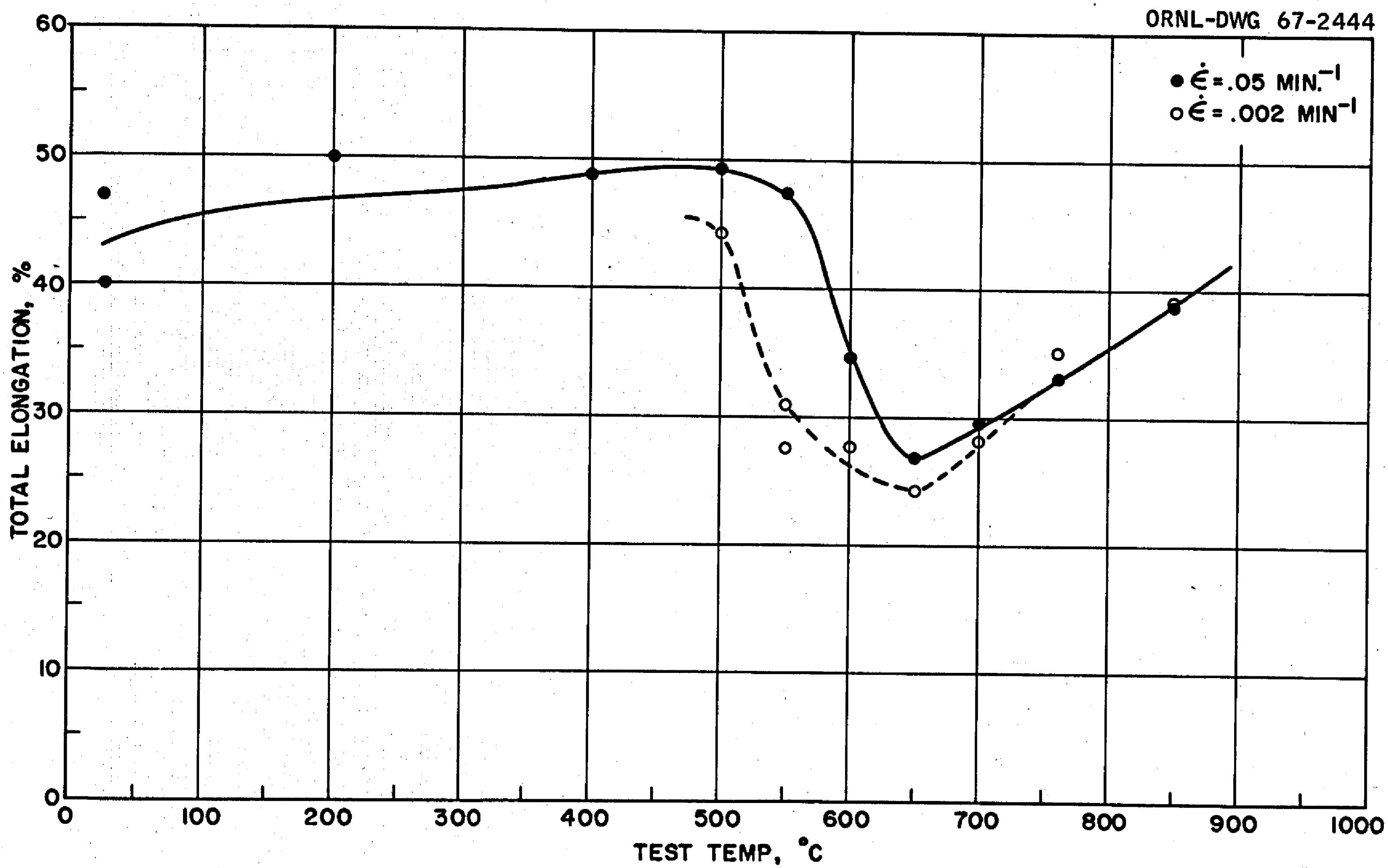

Fig. 10. Tensile Ductilities of MSRE Surveillance Control Specimens, Heat 5085.

Table 5. Results of Tensile Tests on MSRE Surveillance Specimens
Heat 5085

Specimen Number	Test Temperature (°C)	Strain Rate (min^{-1})	Stress (psi)		Elongation (%)		Reduction in Area (%)	True Fracture Strain (%)
			Yield	Ultimate	Uniform	Total		
C-27	25	2	62,300	101,500	25.6	28.4	17.1	19.0
A-25	25	0.5	50,200	95,600	26.7	27.3	19.7	22.0
A-16	25	0.05	48,100	100,300	34.3	34.5	26.0	30.1
A-15	200	0.05	39,500	94,100	37.8	38.6	28.2	33.3
A-26	400	0.05	35,700	87,300	35.0	36.0	26.3	30.6
A-9	500	0.05	34,900	87,900	42.2	42.8	33.9	40.0
B-23	500	0.002	34,000	71,600	21.9	23.1	27.9	32.6
B-1	550	0.05	42,000	74,000	19.6	20.0	18.7	20.9
B-5	550	0.002	33,700	55,100	10.4	12.7	14.7	15.9
B-26	600	0.05	32,500	62,000	18.2	19.6	21.7	24.5
B-4	600	0.002	32,300	52,000	11.1	12.0	12.5	13.5
B-19	650	0.05	32,000	52,800	12.6	13.7	13.9	15.0
B-6	650	0.002	32,100	42,900	6.5	9.4	7.9	8.1
C-20	700	0.05	29,900	43,600	9.3	12.3	5.6	9.4
C-1	700	0.002	37,800	43,100	2.4	2.8	5.9	5.9
B-2	760	0.05	28,900	41,100	8.0	8.5	10.0	10.5
C-21	760	0.002	28,010	33,700	2.4	3.5	2.3	2.0
B-20	850	0.05	27,900	31,400	2.5	3.8	0.65	0.20
C-8	850	0.002	20,600	20,600	0.8	1.8	1.3	0.60

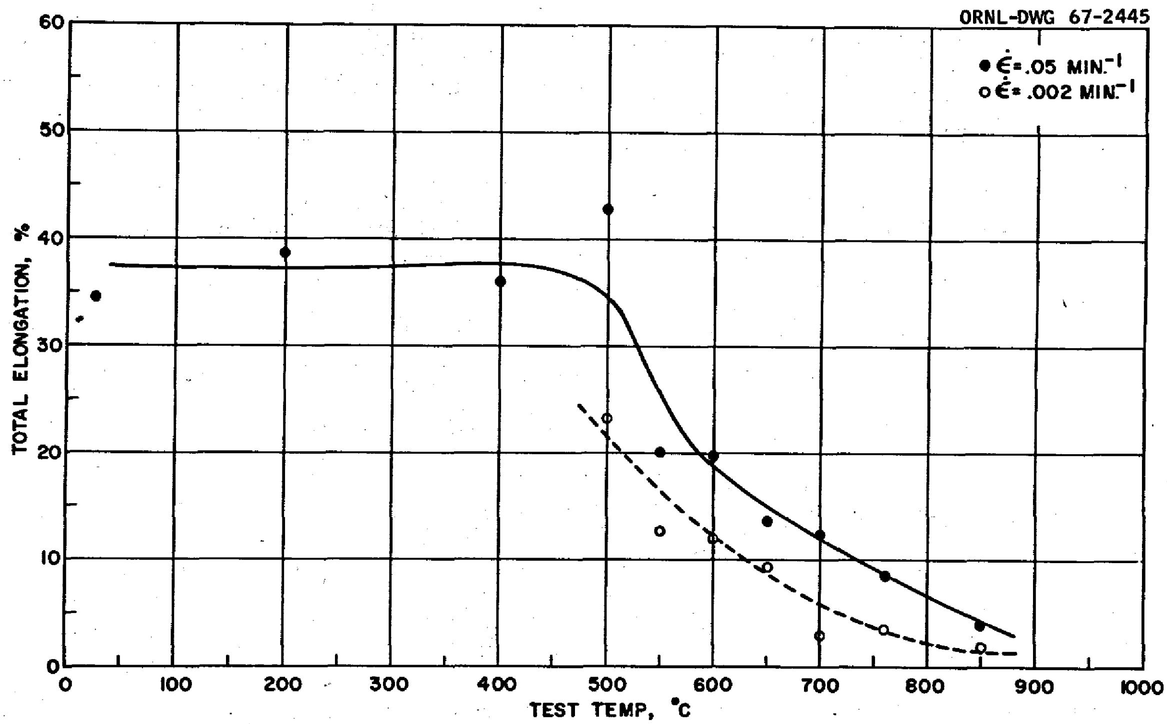

Fig. 11. Tensile Ductilities of MSRE Surveillance Specimens, Heat 5085.

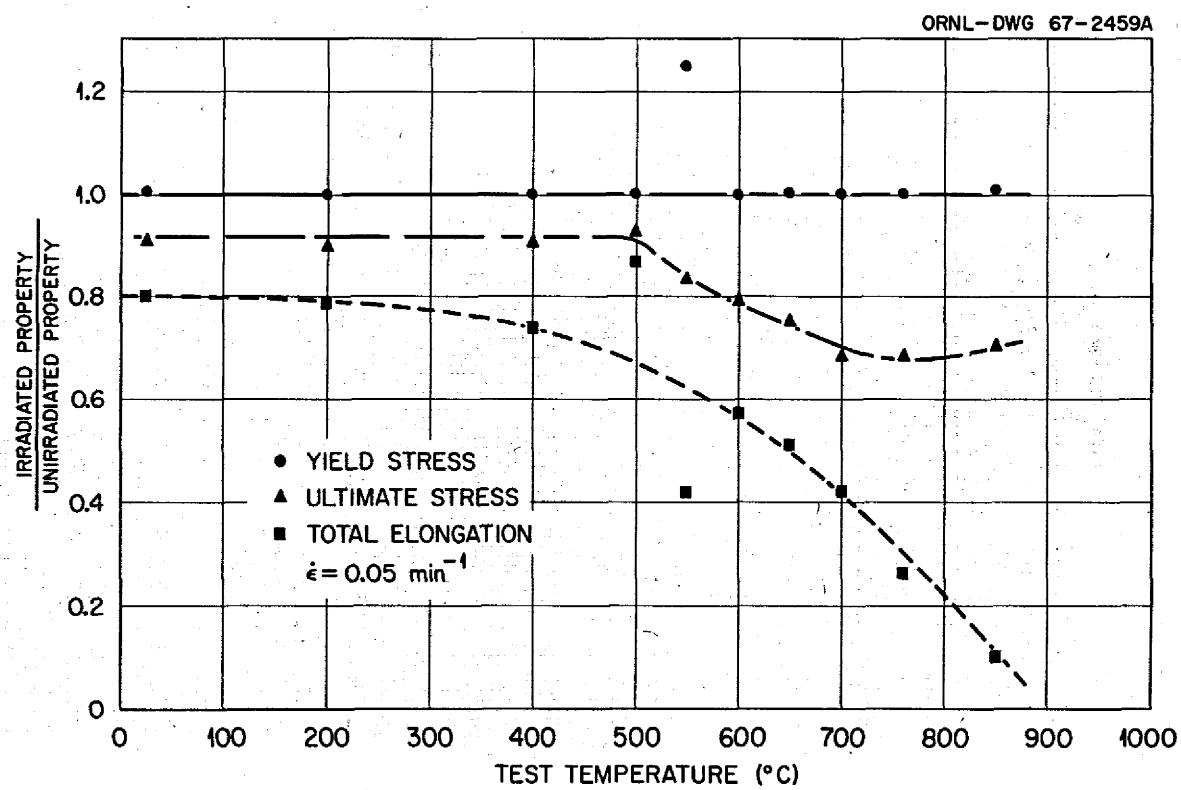

Fig. 12. Comparative Tensile Properties of Irradiated and Unirradiated MSRE Surveillance Specimens, Heat 5085.

The elongations at failure for the two heats of material are compared in Figs. 13 and 14. At a strain rate of 0.05 min^{-1} (Fig. 13) there are several minor variations in the ductilities of the control specimens. The main difference is that the ductility of heat 5085 is consistently lower up to about 500°C. Both heats of the surveillance specimens exhibit a reduction in ductility at a test temperature of 25°C; however, the reduction is greater for heat 5085. The ductility of heat 5081 recovers some with increasing test temperature, but heat 5085 maintains its reduced ductility. Above about 500°C the ductility of the controls drops rapidly, but the ductility of the irradiated surveillance specimens decreases more rapidly. Both heats have very similar ductilities at temperatures above 600°C. The ductilities of the two heats at a strain rate of 0.002 min^{-1} are compared in Fig. 14. The control specimens of both heats exhibited very similar ductilities, the characteristic ductility minimum being exhibited. The irradiated surveillance specimens have much lower ductilities, but the values are very similar for the two heats.

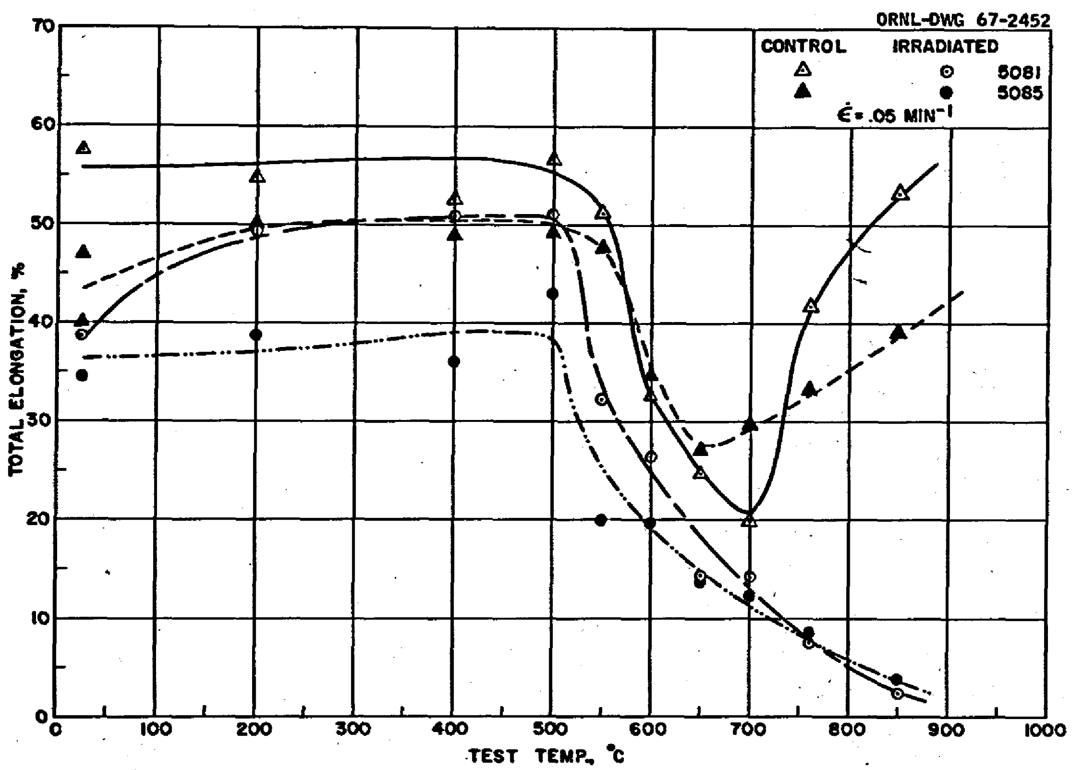

Fig. 13. Comparative Tensile Ductilities of MSRE Surveillance Specimens and Their Controls at a Strain Rate of 0.05 min^{-1}.

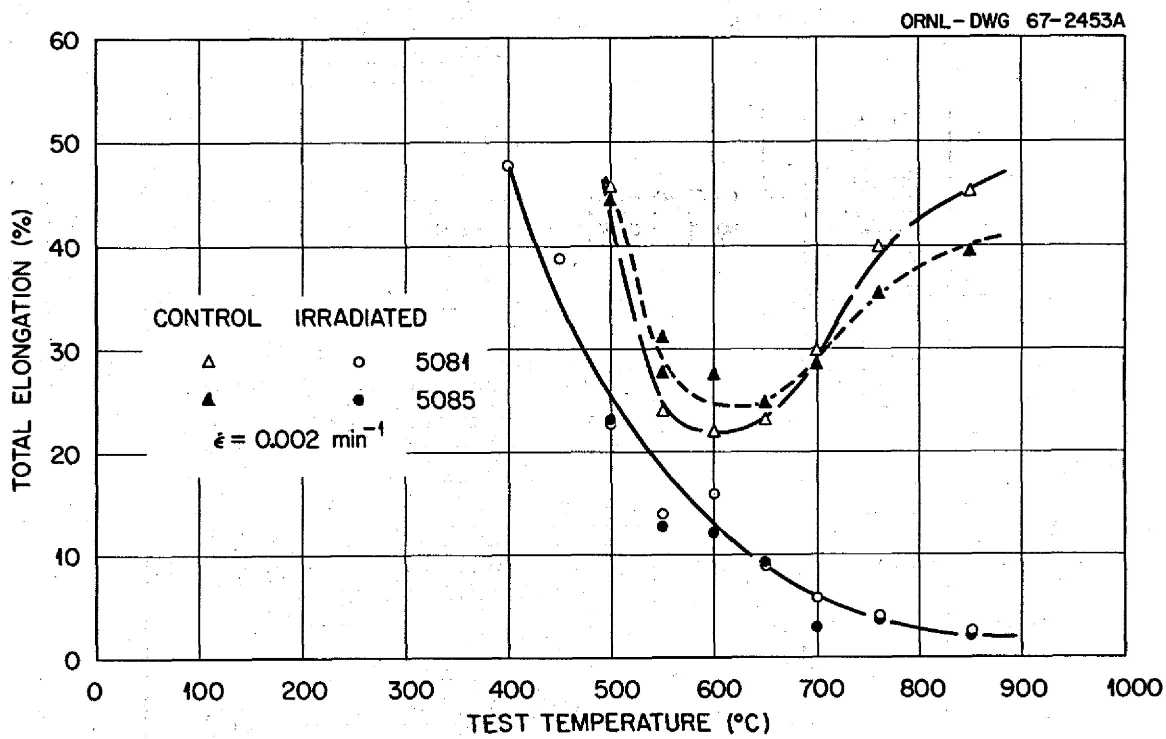

Fig. 14. Comparative Tensile Ductilities of MSRE Surveillance Specimens and Their Controls at a Strain Rate of 0.002 min^{-1}.

We took a brief look at how the tensile properties of the material varied as a function of heat treatment in the unirradiated state. The properties of heat 5081 in several metallurgical conditions are given in Table 6. The anneal for 2 hr at 900°C generally decreased the strength and increased the rupture strain over that of the as-received material. One exception to this behavior is an increase in ultimate stress at 650°C due to the 2 hr anneal at 900°C. The exposure to molten salt at 650°C for 4800 hr caused a decrease in the ductility and slight variations in the strength. The tensile properties of heat 5085 in the unirradiated condition are given in Table 7. The properties of this heat are not significantly different in the as-received condition and after annealing 2 hr at 900°C. The exposure to molten salt at 650°C caused a general decrease of 10 to 20% in the rupture ductility, but the strength was not affected significantly.

The postirradiation tensile properties of several heats of MSRE material are compared in Table 8. The first two sets of data for heat 5065 show that the postirradiation properties were not affected by

Table 6. Tensile Properties of Unirradiated Hastelloy N Heat 5081

Specimen Number	Test Temperature (°C)	Strain Rate (min^{-1})	Stress (psi) Yield	Stress (psi) Ultimate	Elongation (%) Uniform	Elongation (%) Total	Reduction in Area (%)
			As-received				
5006	25	0.05	77,400	130,600	44.9	46.9	48.0
5005	500	0.05	38,200	103,300	53.3	55.3	34.0
5004	500	0.002	40,000	103,200	51.2	52.6	41.5
5008	650	0.05	39,100	73,400	18.0	19.8	19.1
5007	650	0.002	38,200	65,100	14.4	15.2	15.8
			Annealed 2 hr at 900°C				
4300	25	0.05	52,600	125,300	56.7	59.5	50.5
4303	500	0.05	32,000	100,300	57.8	60.7	44.4
4301	650	0.05	32,200	81,800	31.7	33.9	29.9
4302	650	0.002	32,900	74,900	29.0	29.5	31.8
			Annealed 2 hr at 900°C plus 4800 hr in MSRE salt at 650°C				
AC-8	25	0.05	47,700	118,700	55.9	57.6	48.8
AC-19	500	0.05	35,800	97,800	53.6	56.6	46.2
BC-9	500	0.002	36,200	95,300	46.2	47.0	38.1
AC-27	650	0.05	32,400	68,400	23.8	24.6	23.1
AC-17	650	0.002	33,600	66,700	22.8	23.2	21.6

Table 7. Tensile Properties of Unirradiated Hastelloy N
Heat 5085

Specimen Number	Test Temperature (°C)	Strain Rate (min^{-1})	Stress (psi) Yield	Stress (psi) Ultimate	Elongation (%) Uniform	Elongation (%) Total	Reduction in Area (%)
			As-received				
76	25	0.05	52,200	116,400	51.3	52.5	56.3
77	427	0.05	30,700	102,900	57.6	59.4	49.9
284	600	0.02	32,200	85,100	46.6	47.6	40.4
78	650	0.05	28,700	80,700	35.5	36.7	33.2
285	650	0.02	31,900	65,000	25.8	31.8	27.2
283	650	0.002	30,500	64,300	22.6	24.1	28.8
79	760	0.05	32,100	61,500	24.7	27.0	31.9
80	871	0.05	30,700	42,300	9.0	31.8	33.4
81	982	0.05	23,100	23,100	1.8	40.2	43.9
			Annealed 2 hr at 900°C				
4295	25	0.05	51,500	120,800	52.3	53.1	42.2
4298	500	0.05	32,600	94,800	51.2	54.1	40.9
4299	500	0.002	33,500	100,200	52.0	53.3	41.7
4296	650	0.05	29,600	75,800	31.7	33.7	34.6
			Annealed 2 hr at 900°C plus 4800 hr in MSRE salt at 650°C				
FC-3	25	0.05	45,500	111,200	46.8	46.8	31.5
DC-19	500	0.05	33,600	94,300	48.8	49.3	41.5
DC-26	500	0.002	33,400	91,700	43.3	44.3	37.8
DC-14	650	0.05	31,800	70,100	25.8	26.8	30.0
DC-25	650	0.002	31,500	62,500	22.8	24.3	27.2

Table 8. Postirradiation Tensile Properties[a] of Several Heats of MSRE Hastelloy N

Specimen Number	Heat Number	Boron Level (ppm)	Irradiation Temperature (°C)	Thermal Dose (neutrons/cm^2)	Test Temperature (°C)	Strain Rate (min^{-1})	Stress (psi) Yield	Stress (psi) Ultimate	Elongation (%) Uniform	Elongation (%) Total	Reduction in Area (%)
				$\times 10^{20}$							
Experiment ORR-149											
570[b]	5065	20	43	8.5	25	0.05	102,900	135,100	31.5	35.5	52.0
571[b]	5065	20	43	8.5	200	0.05	82,300	119,600	36.1	39.2	54.8
572[b]	5065	20	43	8.5	650	0.05	44,600	76,900	26.3	27.3	24.5
574[b]	5065	20	43	8.5	650	0.002	40,800	57,400	12.2	13.1	21.9
573[b]	5065	20	43	8.5	871	0.05	33,500	36,400	1.7	1.8	3.25
575[b]	5065	20	43	8.5	871	0.002	23,200	23,400	0.9	1.8	6.07
581[c]	5065	20	43	8.5	25	0.05	101,500	132,200	30.0	33.6	55.2
582[c]	5065	20	43	8.5	200	0.05	78,600	118,300	37.3	39.8	45.9
583[c]	5065	20	43	8.5	650	0.05	35,100	77,700	25.3	25.8	22.6
585[c]	5065	20	43	8.5	650	0.002	38,100	66,200	13.7	14.3	17.3
584[c]	5065	20	43	8.5	871	0.05	37,100	38,500	1.7	1.9	2.94
586[c]	5065	20	43	8.5	871	0.002	25,900	25,900	0.8	1.6	5.26
Experiment ORR-155											
2289[b]	5067	20	500–700	1.4	25	0.05	59,000	123,700	49.4	51.2	45.4
2290[b]	5067	20	500–700	1.4	650	0.05	38,400	66,800	14.0	14.0	20.5
2291[b]	5067	20	500–700	1.4	650	0.002	36,400	59,900	9.6	9.6	16.0
2285[b]	5085	38	500–700	1.4	25	0.05	46,300	110,600	41.1	41.2	40.3
2286[b]	5085	38	500–700	1.4	650	0.05	30,800	64,400	18.0	21.2	19.1
2287[b]	5085	38	500–700	1.4	650	0.002	30,200	51,800	9.3	9.9	15.4
1857[b]	5065	20	500–700	1.4	25	0.05	50,100	117,000	54.4	56.1	53.2
1858[b]	5065	20	500–700	1.4	650	0.05	37,400	62,100	12.3	12.4	17.2
1859[b]	5065	20	500–700	1.4	650	0.002	34,800	49,100	6.4	6.5	15.3
Experiment ETR-41-31											
1273[b]	5065	20	600 ± 100	3.5	550	0.002	49,100	68,600	9.1	9.4	14.7
1276[b]	5065	20	600 ± 100	3.5	600	0.002	42,200	56,300	8.2	8.5	11.7
1270[b]	5065	20	600 ± 100	3.5	650	0.05	41,200	59,000	10.8	11.3	14.7
1271[b]	5065	20	600 ± 100	3.5	650	0.002	42,600	51,800	5.9	6.1	10.2
1274[b]	5065	20	600 ± 100	3.5	760	0.002	41,900	46,000	2.8	2.8	5.6
Experiment ETR-41-30											
383[b]	5065	20	<150	5	650	0.05	46,700	76,200	21.6	22.2	28.8
380[b]	5065	20	<150	5	650	0.002	37,700	53,300	9.3	10.0	10.1
384[b]	5065	20	<150	5	650	0.002	40,000	57,500	11.4	11.6	17.5
Experiment MSRE											
D-16[d]	5081	50	650	1.3	25	0.05	51,100	105,500	38.5	38.7	31.3
E-7[d]	5081	50	650	1.3	650	0.05	34,600	57,200	13.8	14.3	13.9
E-14[d]	5081	50	650	1.3	650	0.002	34,400	48,400	8.2	9.0	11.6
A-16[d]	5085	38	650	1.3	25	0.05	48,100	100,300	34.3	34.5	26.0
B-19[d]	5085	38	650	1.3	650	0.05	32,000	52,800	12.6	13.7	13.9
B-6[d]	5085	38	650	1.3	650	0.002	32,100	42,900	6.5	9.4	7.9

[a] Irradiated in a helium environment except for specimens from MSRE.
[b] As received.
[c] Annealed 8 hr at 871°C.
[d] Annealed 2 hr at 900°C.

whether the material was irradiated in the as-received condition or whether it was annealed 8 hr at 871°C. These specimens were irradiated at 43°C, and the ductilities at 25°C (0.05 min^{-1}) and 650°C (0.002 min^{-1}) were 34 to 36 and 13 to 14%, respectively. When irradiated at an elevated temperature, this same heat had elongations at 650°C (0.002 min^{-1}) of 6.5 and 6.1%. Heats 5067 and 5085 showed somewhat better ductilities at 650°C (0.002 min^{-1}) with values of 9 to 10% being obtained for irradiations at elevated temperatures. The ductilities of the two surveillance heats at 650°C agree closely with those observed previously for heats 5085 and 5067. However, the room temperature ductilities are lower than those observed for any heat of material irradiated at an elevated temperature. Heat 5081 was included in another experiment in the Oak Ridge Research Reactor,[6] and the results are compared with those for the MSRE surveillance specimens in Fig. 15. These results indicate that the properties of the material are unaffected by the salt environment.

---

[6]W. R. Martin and J. R. Weir, "Effect of Elevated Temperature Irradiation on the Strength and Ductility of the Nickel-Base Alloy, Hastelloy N," Nucl. Appl. 1(2), 160–67 (1965).

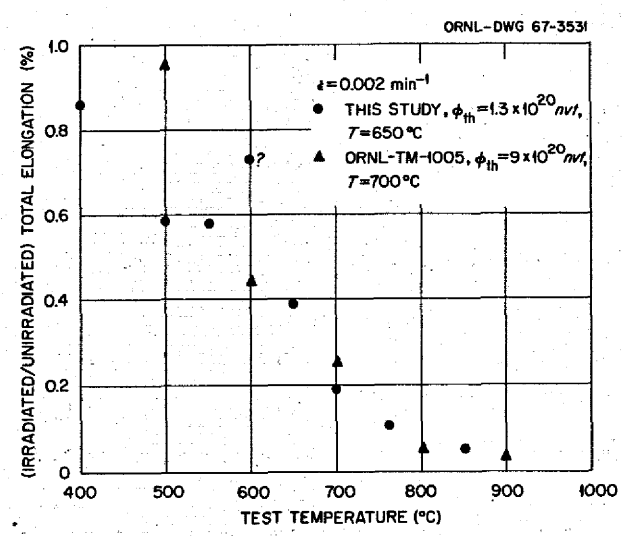

Fig. 15. Comparative Effects of Irradiation in MSRE and ORR on the Ductility of Hastelloy N, Heat 5081.

We also ran several creep-rupture tests on the irradiated materials to evaluate their properties under creep conditions. For comparison, the results of several creep-rupture tests on unirradiated heat 5081 are given in Table 9. Of the two heat treatments investigated, 2 hr at 900°C and the surveillance control treatment, the latter resulted in slightly lower rupture strains. The creep-rupture data are plotted in Fig. 16, and the MSRE surveillance control specimens exhibit a slightly reduced rupture life. However, the minimum creep rate is the same after the two heat treatments (Fig. 17).

Table 9. Creep-Rupture Properties of Unirradiated Hastelloy N at 650°C
Heat 5081

Test Number	Stress (psi)	Rupture Life (hr)	Rupture Strain (%)	Reduction in Area (%)	Minimum Creep Rate (%/hr)
		Annealed 2 hr at 900°C			
6159	70,000	5.1	35.0	12.8	2.1
6155	55,000	71.8	33.9	29.2	0.26
6156	47,000	76.0	12.4	27.0	0.091
6157	40,000	648.3	42.5	25.2	0.032
6158	32,400	2133.3	46.8	20.1	0.012
6160[a]	27,000	2349.0	10.2	3.7	0.0047
		Annealed 2 hr at 900°C plus 4800 hr at 650°C in MSRE salt			
6077	55,000	40.7	24.3	21.9	0.25
6075	47,000	147.9	27.2	21.9	0.098
6076	40,000	321.0	31.1	26.7	0.061
6071	32,400	848.0	16.5	16.1	0.014

[a]Discontinued prior to failure.

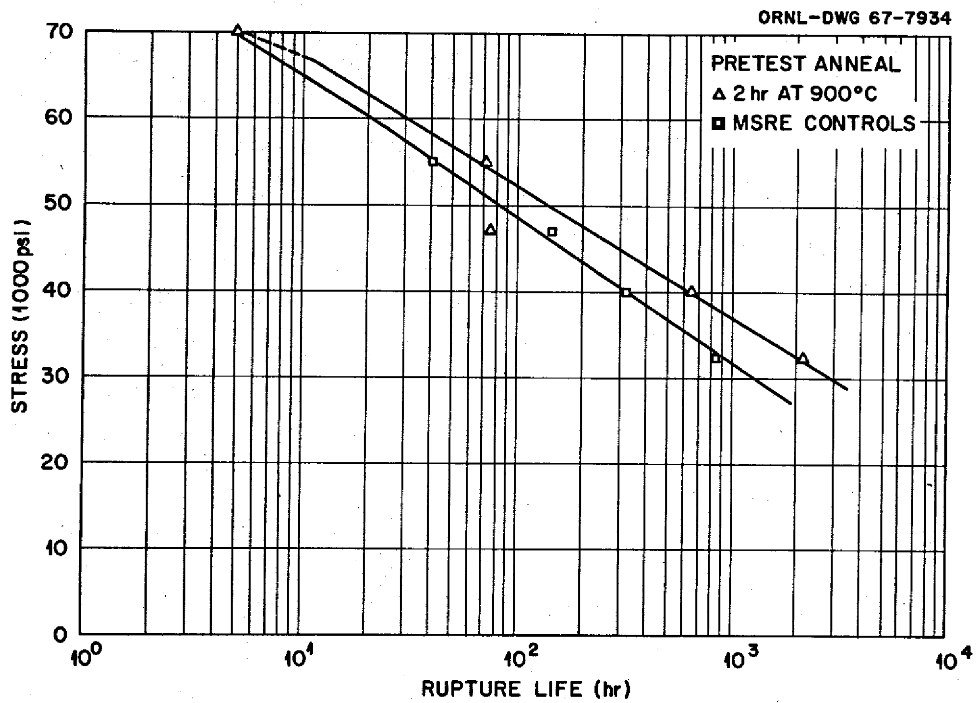

Fig. 16. Creep-Rupture Properties of Hastelloy N at 650°C, Heat 5081.

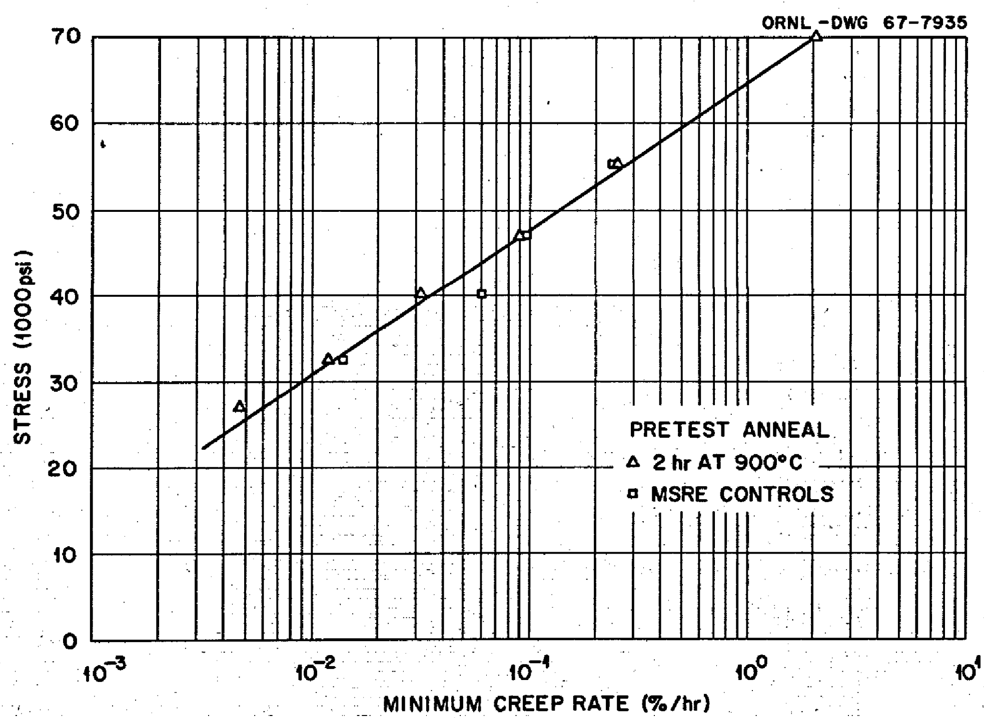

Fig. 17. Minimum Creep Rate of Hastelloy N at 650°C, Heat 5081.

The creep-rupture properties of heat 5085 were investigated in three conditions — as-received, annealed 2 hr at 900°C, and 2 hr at 900°C plus 4800 hr in molten salt (Table 10). The rupture strain of the as-received material is improved by annealing at 900°C, but the long aging treatment at 650°C brings about a slight reduction in the fracture ductility. Figure 18 compares the rupture life after the various heat treatments. The pattern is the same as that for the ductility with the minimum strength being observed for the as-received material and the maximum for the material annealed 2 hr at 900°C. However, the minimum creep rate was unaffected by heat treatment (Fig. 19).

Table 10. Creep-Rupture Properties of Unirradiated Hastelloy N at 650°C
Heat 5085

Test Number	Stress (psi)	Rupture Life (hr)	Rupture Strain (%)	Reduction in Area (%)	Minimum Creep Rate (%/hr)
			As-received		
3792	70,000	0.4	28.0	21.9	9.0
3710	55,000	10.8	10.9	13.3	0.27
3781	47,000	48.6	12.5	14.6	0.086
3713	40,000	179.5	10.9	5.6	0.024
3714	40,000	215.7	14.0	5.6	0.024
3975	30,000	672.6	6.3	6.4	0.006
3795	30,000	1030.0	9.4	7.1	0.006
			Annealed 2 hr at 900°C		
6153	70,000	4.1	32.6	30.7	2.1
6149	55,000	49.5	22.6	30.8	0.26
6150	47,000	246.8	38.5	28.9	0.084
6151	40,000	725.1	37.6	18.4	0.029
6152	32,400	2386.0	37.7	19.9	0.009
6154[a]	27,000	2445.0	9.0	4.0	0.0035
			Annealed 2 hr at 900°C plus 4800 hr at 650°C in MSRE salt		
6074	55,000	20.5	20.8	21.9	0.30
6073	47,000	124.6	31.2	22.9	0.080
6072	40,000	513.3	22.3	19.7	0.029
6070	32,400	2054.6	26.7	16.7	0.0082

[a]Discontinued prior to failure.

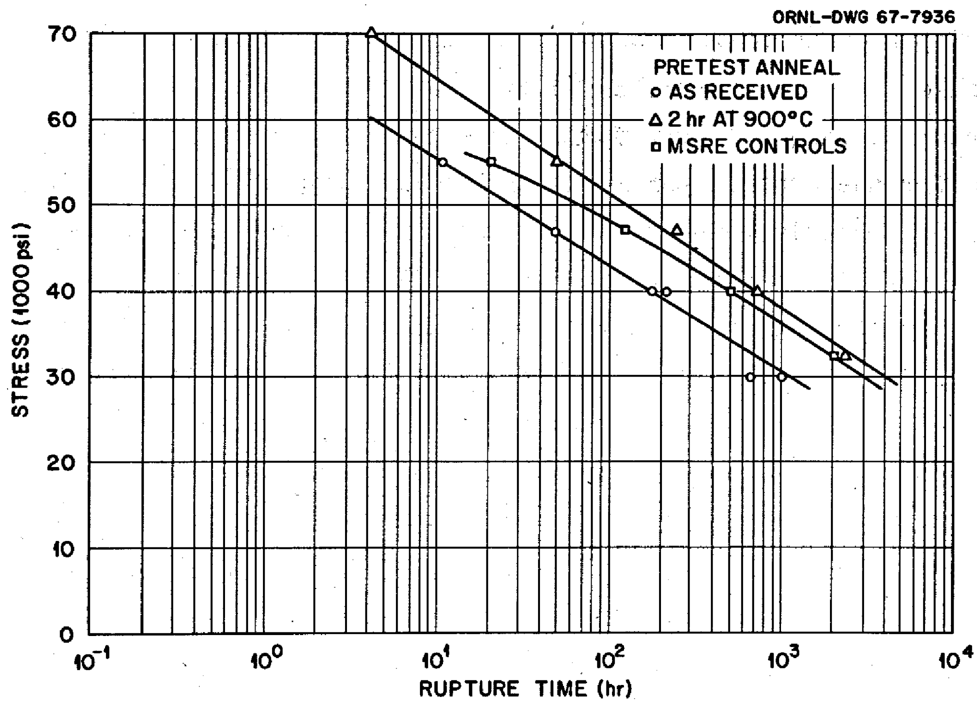

Fig. 18. Creep-Rupture Properties of Hastelloy N at 650°C, Heat 5085.

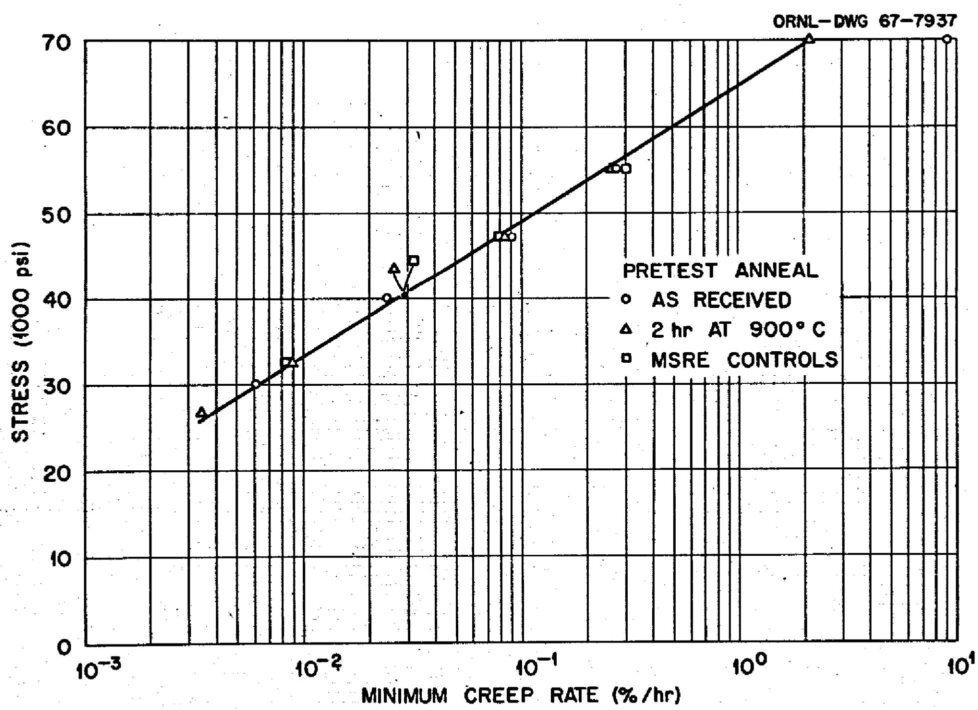

Fig. 19. Minimum Creep Rate of Hastelloy N at 650°C, Heat 5085.

The results of the tests on the surveillance specimens are given in Table 11. The properties (ductility and strength) of heat 5081 are superior to those of heat 5085. However, a comparison of these data with those for the control specimens in Tables 9 and 10 shows that irradiation has significantly reduced the rupture life and ductility of both heats. The rupture lives are compared in Fig. 20 for both heats of material in the irradiated and unirradiated conditions. The effect of irradiation is greater as the stress level increases. The minimum creep rates of the two heats of material in the irradiated and unirradiated conditions are compared in Fig. 21. This parameter appears to be independent of the variables being studied with the possible exception of the irradiated specimens exhibiting a higher strain rate at the 47,000-psi stress level.

Table 11. Postirradiation Creep-Rupture Properties of MSRE Surveillance Specimens[a] at 650°C

Test Number	Heat Number	Stress (psi)	Rupture Life (hr)	Rupture Strain (%)	Reduction in Area (%)	Minimum Creep Rate (%/hr)
R-230	5085	47,000	0.8	1.45	10.0	0.81
R-266	5085	40,000	24.2	1.57	9.7	0.031
R-267	5085	32,400	148.2	1.05	6.5	0.006
R-250	5085	27,000	25.2	1.86	2.2	0.004
R-229	5081	47,000	8.7	2.28	9.2	0.20
R-231	5081	40,000	98.7	2.65	5.8	0.017
R-226	5081	32,400	474.0	3.78	4.0	0.0059
R-233	5081	27,000	2137.1	4.25	0.58	0.0009

[a]Annealed 2 hr at 900°C prior to irradiation.

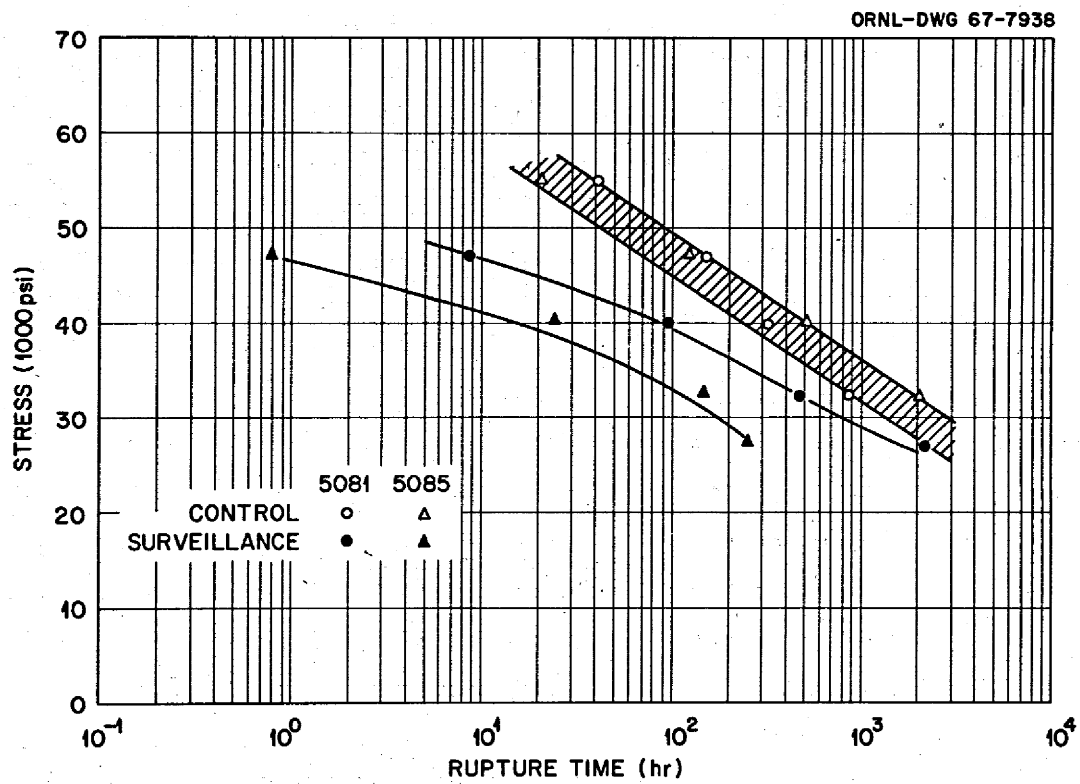

Fig. 20. Comparative Creep-Rupture Properties of Surveillance and Control Specimens at 650°C.

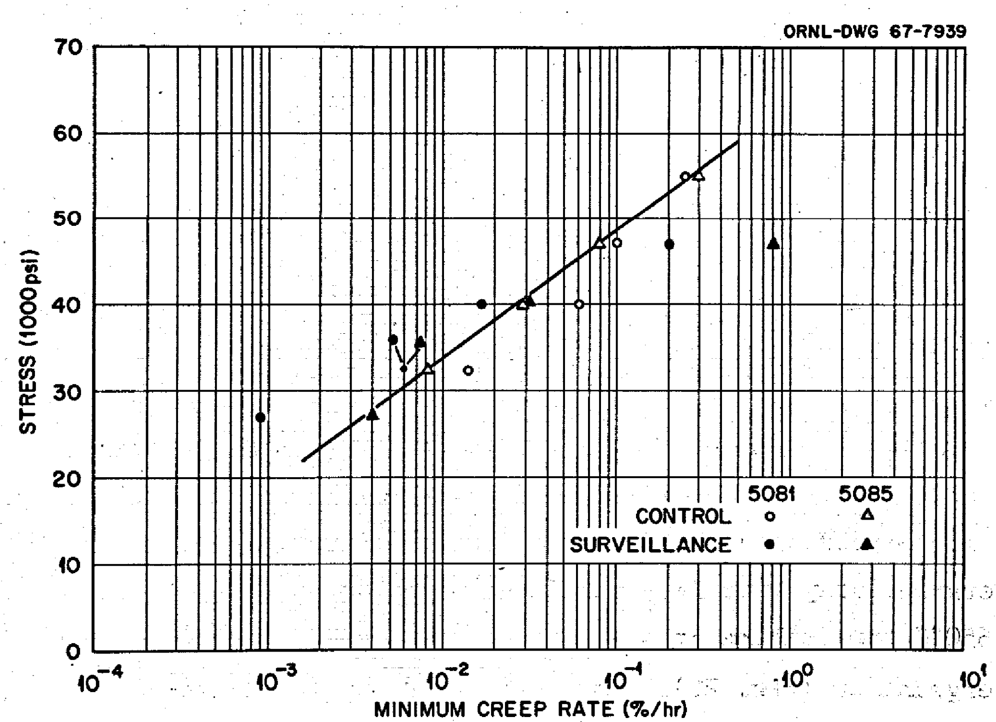

Fig. 21. Comparative Creep Rates for Surveillance and Control Specimens at 650°C.

The results of the creep-rupture tests on the surveillance specimens were compared with data which we had obtained on the "MSRE materials" in other irradiation experiments in the ORR. The results used in this comparison are given in Table 12. The creep-rupture lives are compared in Fig. 22. The data for heat 5085 agree quite well with those obtained previously in the ORR for this same heat and several other MSRE heats. However, the results for heat 5081 are slightly superior. The fracture strains for the various heats of irradiated material are compared in Fig. 23. The data indicate a minimum ductility for a rupture life of 1 to 10 hr with ductility increasing with increasing rupture life. A lower ductility of heat 5085 after irradiation in the MSRE is also indicated, although the data scatter will not permit this as an unequivocal conclusion. The superior ductility of heat 5081 and the least ductility of heat 5065 (heat used for the top and bottom heads of MSRE) are clearly illustrated.

Since transients may occur in which the material is strained at some temperature other than the operating temperature (650°C), we ran a series of tests to determine what effect such transients could have on the fracture strain at 650°C. The results of these tests are given in Table 13. The specimens were strained at other temperatures and then quickly cooled or heated to 650°C and tested to failure. Even though the prestraining treatments carried the specimens as far as 37% of the strain to failure, the strain at 650°C was not decreased. In fact, the prestraining at 760 and 850°C seemed to improve the ability of the material to strain at 650°C.

Several of the specimens were examined metallographically after testing. Figure 24 shows the microstructure of a control specimen from heat 5081 that was tested at 25°C. The specimen has undergone extensive deformation, and the fracture is typical of a transgranular shear-type failure. There is no evidence of intergranular cracking. In contrast, the irradiated specimen from the same heat, shown in Fig. 25, failed intergranularly with less strain and considerable intergranular cracking. At 650°C the failure of the control specimen was predominantly intergranular (Fig. 26). The failure of the surveillance specimen was also intergranular at 650°C with no microstructural evidence of plastic deformation (Fig. 27).

Table 12. Postirradiation Creep-Rupture Properties of Irradiated[a] Hastelloy N at 650°C

Test Number	Thermal Dose (neutrons/cm^2)	Experiment Number	Stress (psi)	Rupture Life (hr)	Rupture Strain (%)	Minimum Creep Rate (%/hr)
	$\times 10^{20}$					
			Heat 5065			
R-15	3.0	ORR-138	39,800	2.8	0.59	0.086
R-13	3.0	ORR-138	32,400	62.6	2.23	0.011
R-35	3.0	ORR-138	27,000	765.8	1.75	0.0019
R-12	3.0	ORR-138	21,500	1907.8	2.28	0.0010
R-159	5.2	ORR-148	40,000	28.6	0.98	0.028
R-167	5.2	ORR-148	40,000	13.0	0.46	0.018
R-65	5.2	ORR-148	35,000	17.7	0.60	0.016
R-168	5.2	ORR-148	30,000	117.0	0.66	0.0049
R-215	1.4	ORR-155	32,400	135.7	1.45	0.0083
			Heat 5067			
R-214	1.4	ORR-155	32,400	361.4	2.78	0.0056
			Heat 5085			
R-14	2.0	ORR-140	39,800	6.7	1.90	0.25
R-11	2.0	ORR-140	32,400	49.3	1.61	0.0098
R-41	2.0	ORR-140	27,000	102.8	2.88	0.0023
R-10	2.0	ORR-140	21,500	2625.8	3.70	0.0009
R-206	1.4	ORR-155	32,400	247.6	1.48	0.0055

[a]Irradiation environment: He–1 vol % O_2. All specimens in the as-received condition.

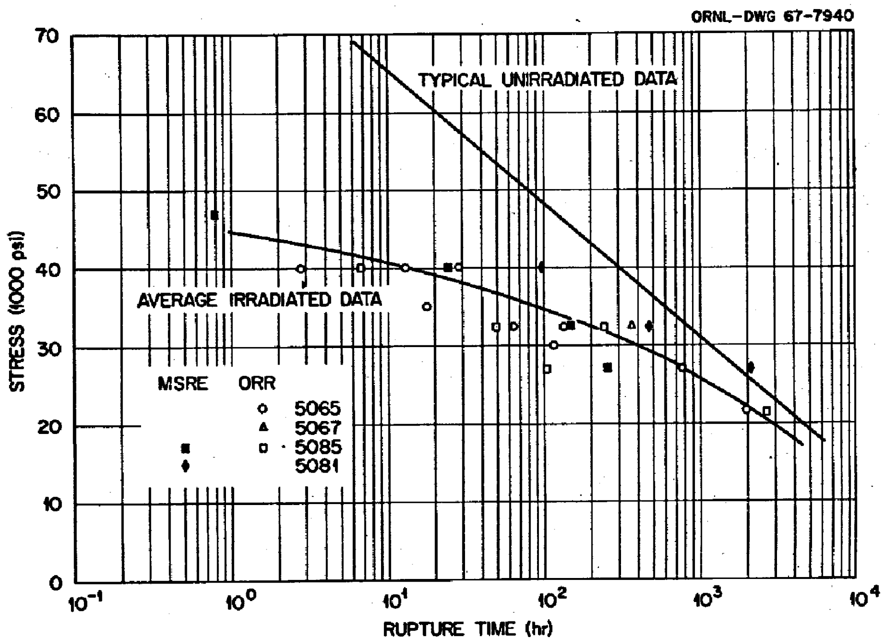

Fig. 22. Comparative Stress-Rupture Properties for Material Irradiated in the MSRE and the ORR at 650°C.

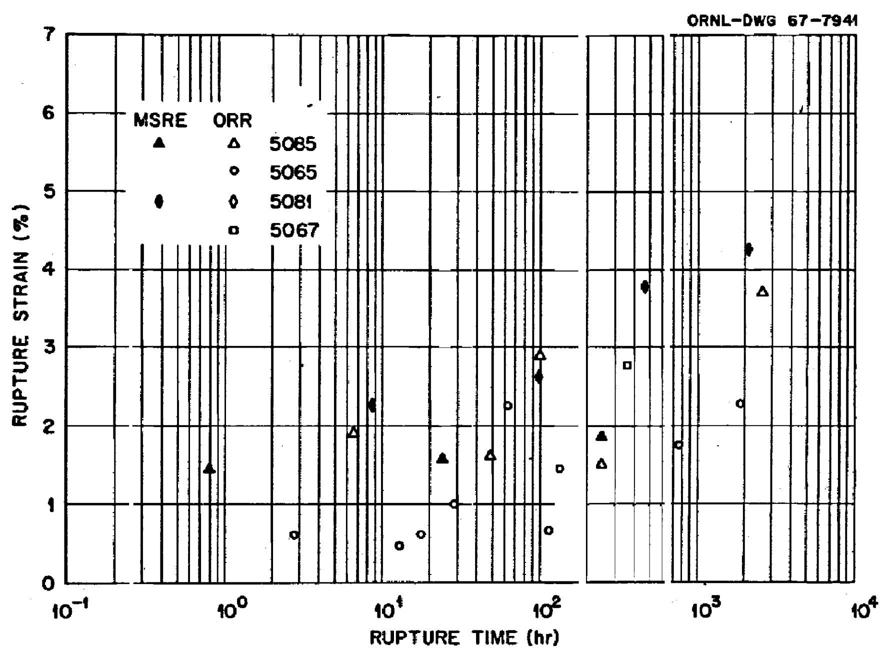

Fig. 23. Comparative Rupture Strains for Irradiated Hastelloy at 650°C.

Table 13. Effects of Prestraining on the Tensile Properties of Hastelloy N Heat 5081[a]

Specimen Number	Pretreatment[b]	Stress (psi)		Elongation[b] (%)		Reduction in Area (%)	True Strain (%)	Fraction of Rupture Strain at Prestraining Temperature (%)
		Yield	Ultimate	Uniform	Total			
E-19	None	34,600	53,000	10.8	11.3	14.6	15.9	
E-14	None	34,400	48,400	8.2	9.0	11.6	12.2	
F-11	Strained 5% at 400°C	45,900	54,700	8.0	10.0	8.2	8.2	10
F-25	Strained 5% at 500°C	47,700	58,300	10.9	11.5	14.2	15.4	20
F-24	Strained 5% at 600°C	47,900	58,500	10.4	11.3	11.0	11.3	32
D-11	Strained 2% at 700°C	40,200	54,000	9.7	10.6	14.2	15.4	37
F-4	Strained 1% at 760°C	35,500	56,400	11.9	12.6	15.5	16.9	26
F-16	Strained 0.5% at 850°C	35,700	59,800	15.2	15.9	13.5	14.7	24

[a]Ruptured at 650°C: Strain rate = 0.002 min^{-1}.

[b]Prestraining carried out at a strain rate of 0.002 min^{-1}.

[c]Includes only the strain at 650°C.

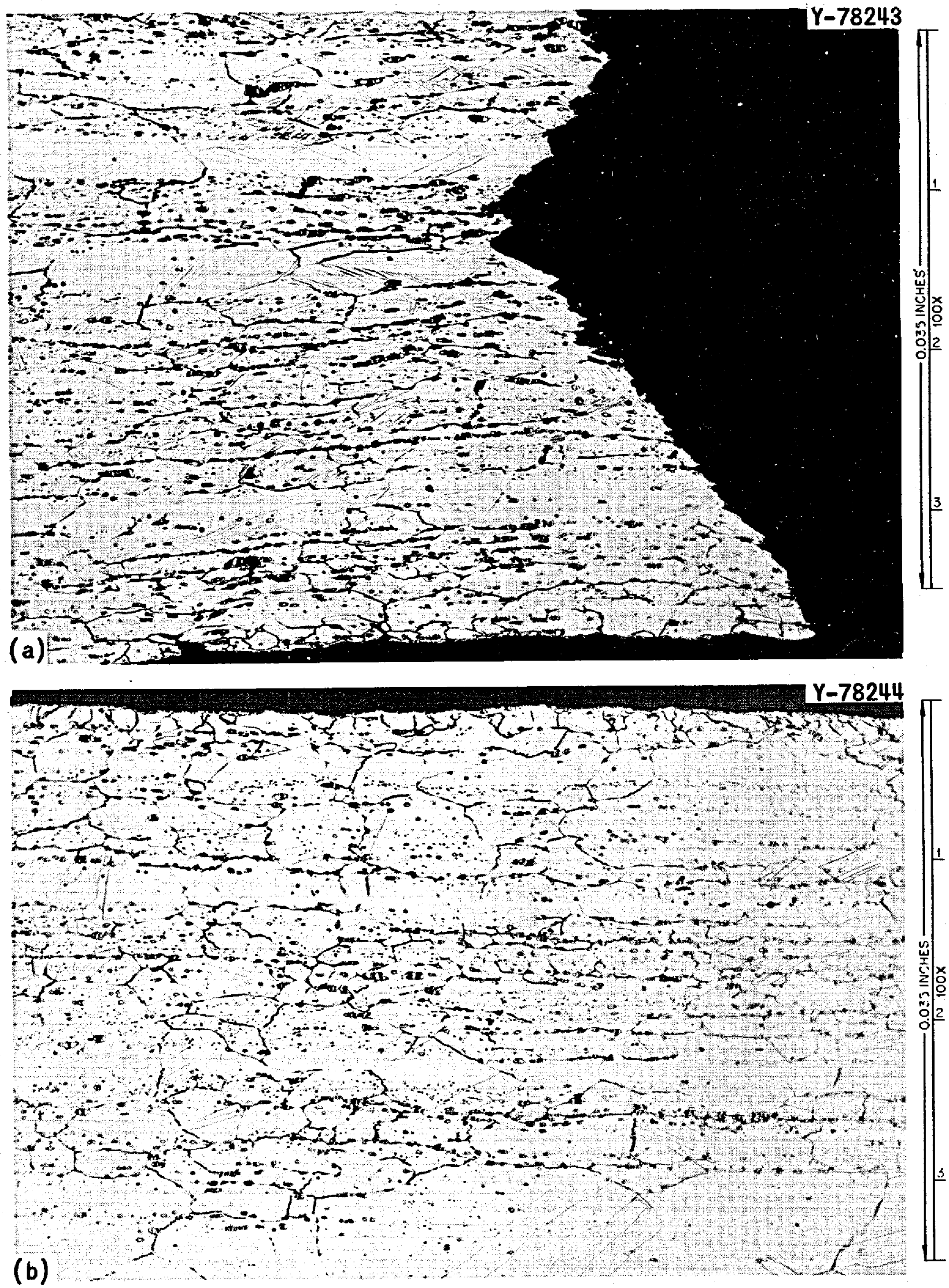

Fig. 24. Photomicrographs of Control Specimen AC-8 from Heat 5081 Tested at 25°C and at a Strain Rate of 0.05 min^{-1}. (a) Fracture. (b) Edge of specimen about 1/4 in. from fracture. Etchant: glyceria regia.

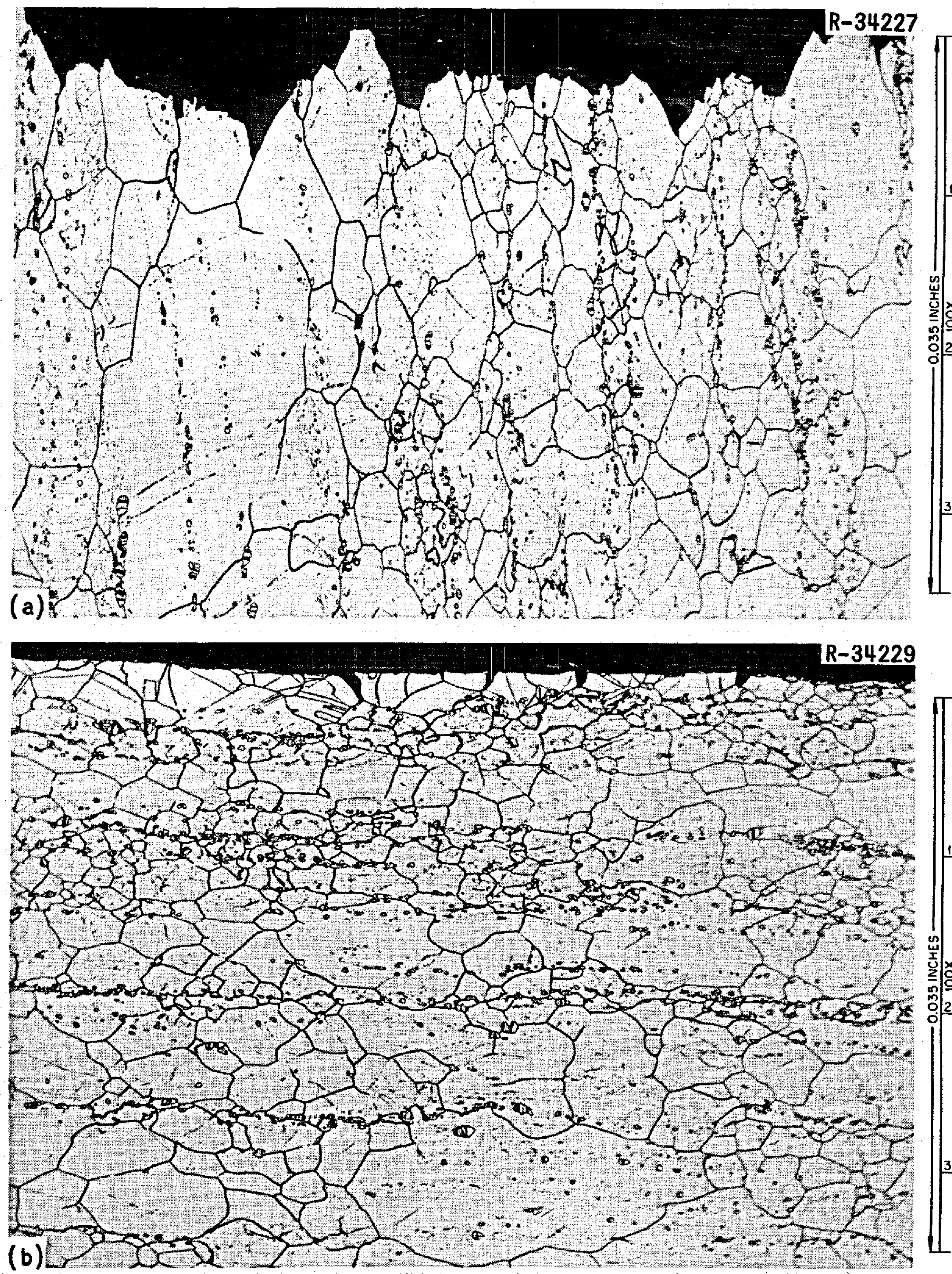

Fig. 25. Photomicrographs of Surveillance Specimen D-16 from Heat 5081 Tested at 25°C and at a Strain Rate of 0.05 min^{-1}. (a) Fracture. (b) Edge of specimen about 1/4 in. from fracture. Etchant: glyceria regia.

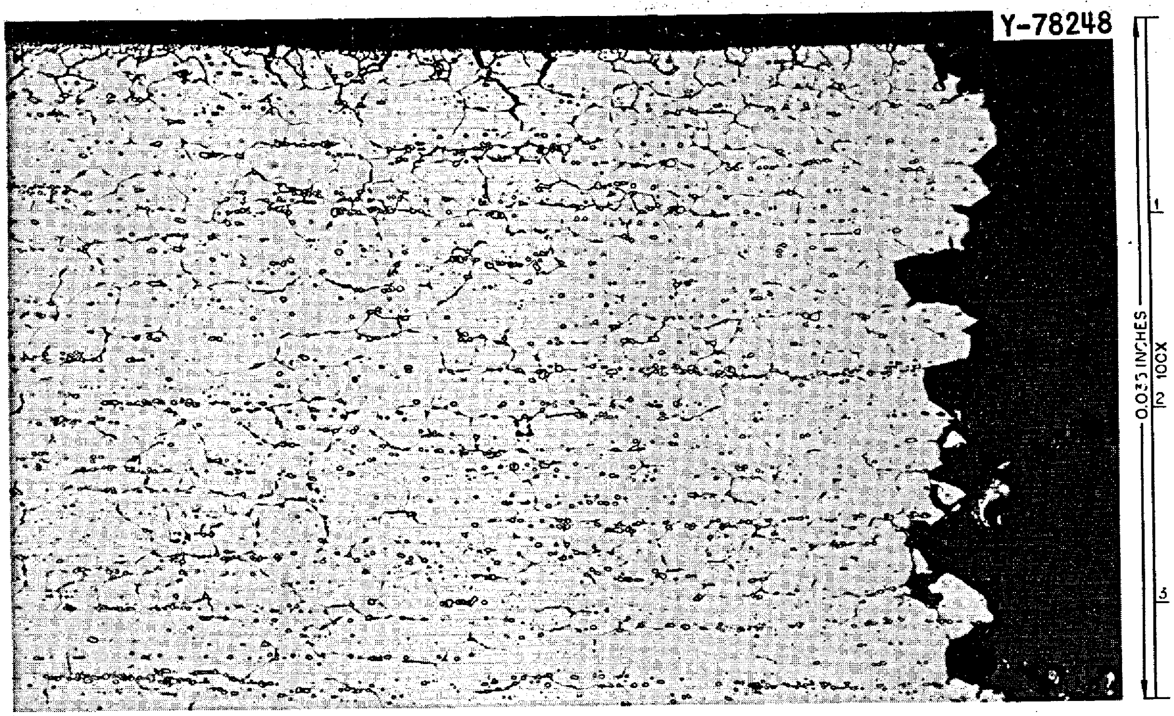

Fig. 26. Photomicrograph of the Fracture of Control Specimen AC-17 from Heat 5081 Tested at 650°C and at a Strain Rate of 0.002 min^{-1}. Etchant: glyceria regia.

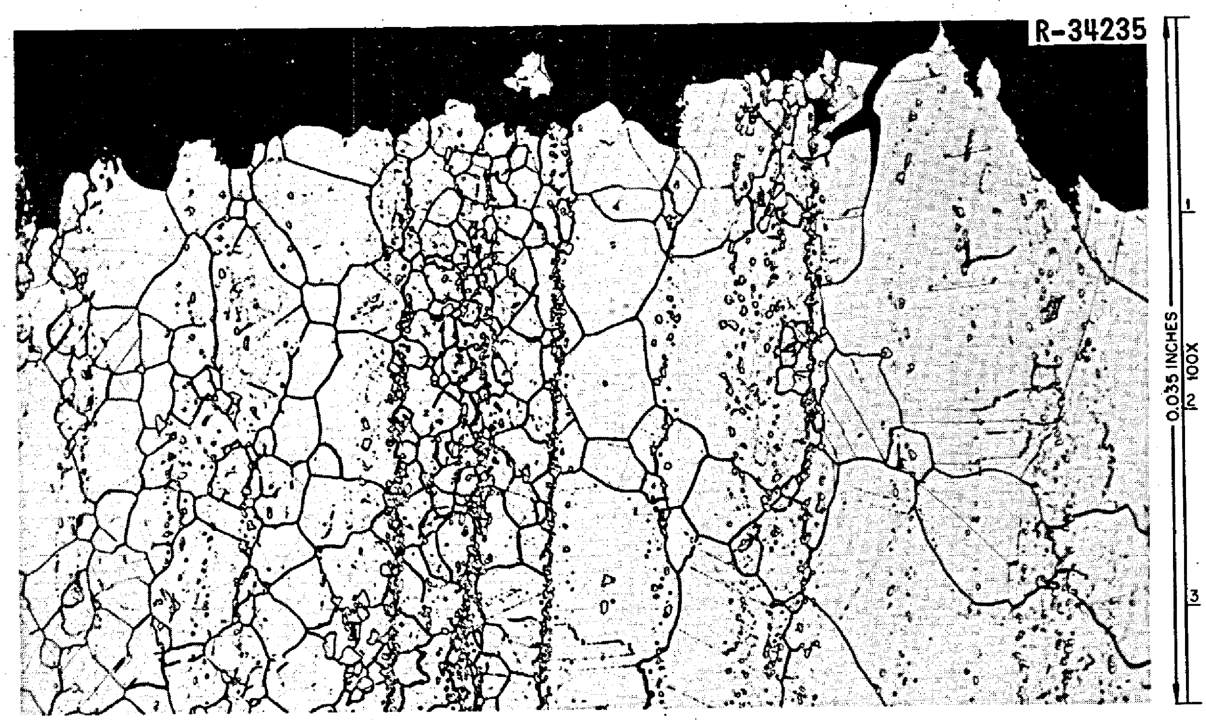

Fig. 27. Fracture of Surveillance Specimen E-14 from Heat 5081 Tested at 650°C and at a Strain Rate of 0.002 min^{-1}. Etchant: glyceria regia.

The failure of the control material from heat 5085 was found to be predominantly intergranular (Fig. 28). However, the elongated grains attest to the large amount of strain that has occurred. The large precipitates have been identified as M_6C, and they normally fracture when strained at temperatures less than about 500°C. The surveillance specimen from heat 5085 tested at 25°C is shown in Fig. 29. The failure is largely intergranular with numerous intergranular cracks in the microstructure. The edge of the specimen (Fig. 29b) is quite clean with no evidence of corrosion or material deposition. However, the part of the specimen that touched the graphite in the surveillance assembly was found to have a reaction product near the surface varying from 1 to 2 mils in depth (Fig. 30). This product was not distributed uniformly around the specimen and varied in form from a lamellar to a rope-like intergranular product. At 650°C the failure of the control specimen was predominantly intergranular (Fig. 31). The surface reaction product observed in specimens from the reactor where they were in contact with the graphite was also noted in the control specimens (Fig. 32). Although the micrographs that have been shown are for heat 5085, the surface reaction was also noted in heat 5081. Electron microprobe examination showed that this layer contained from 0.3 to 1.5 wt % C, indicating that there was some transfer of carbon from the graphite to the Hastelloy N where the two materials were in contact. Figure 33 shows the fracture of the surveillance specimen from heat 5085 that was tested at 650°C. The failure is predominantly intergranular with no metallographic evidence of plastic deformation.

Extraction replicas were made on the surveillance and control specimens. This technique involves depositing carbon on a polished surface of the specimen and then dissolving electrolytically the matrix in a solution of 10% HCl in ethanol until the carbon falls free. The precipitates are not attacked by the solution, and they are held by the carbon. After suitable washing and drying, the replica can be examined in the electron microscope. Transmission electron micrographs can be made as well as selected area diffraction patterns for phase identification. An extraction replica of a control specimen from heat 5081 is shown in Fig. 34. The predominant feature is the relatively large precipitates that have been identified

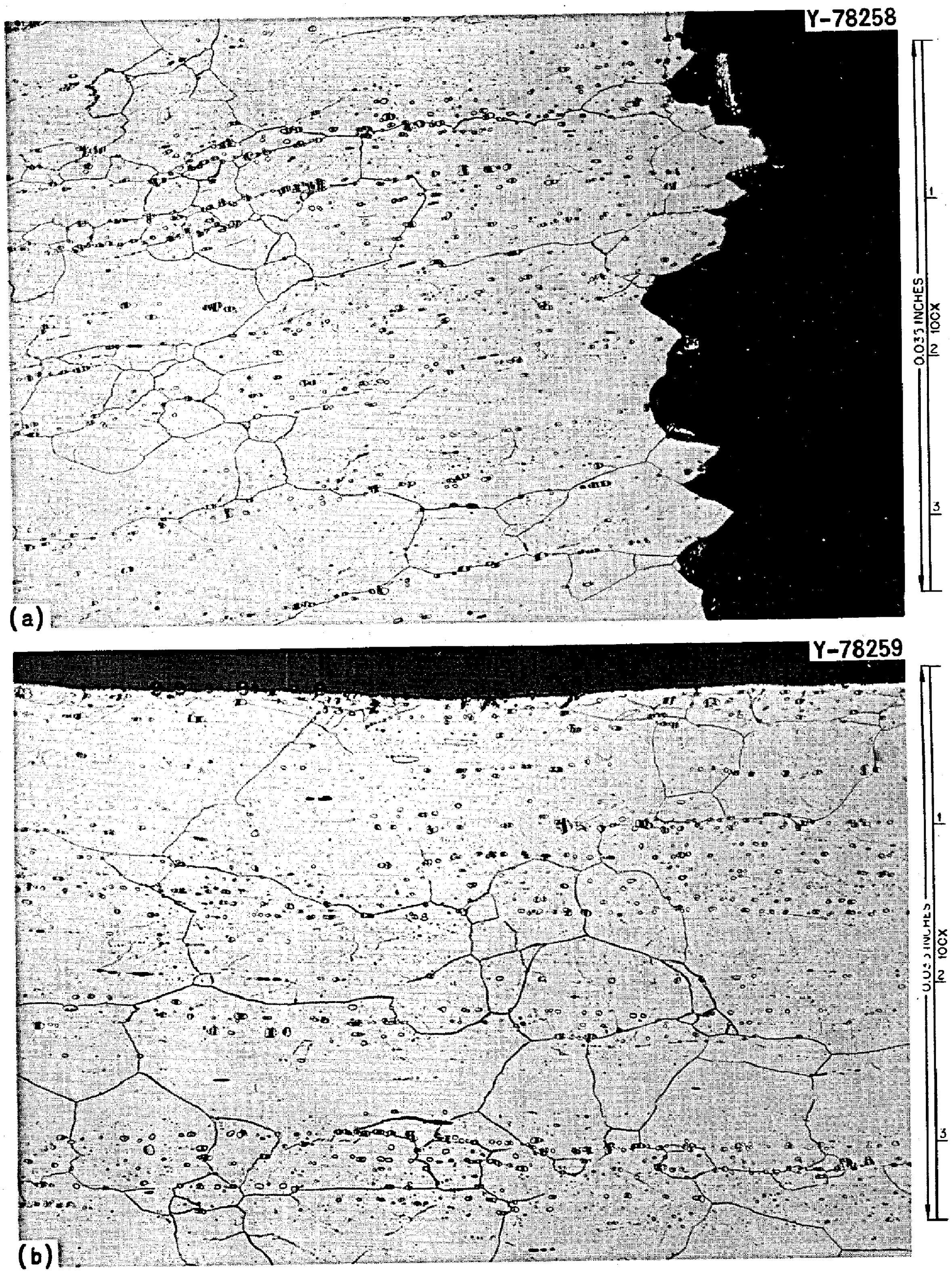

Fig. 28. Photomicrographs of Control Specimen DC-24 from Heat 5085 Tested at 25°C and at a Strain Rate of 0.05 min^{-1}. (a) Fracture. (b) Edge of specimen about 1/4 in. from fracture. Etchant: glyceria regia.

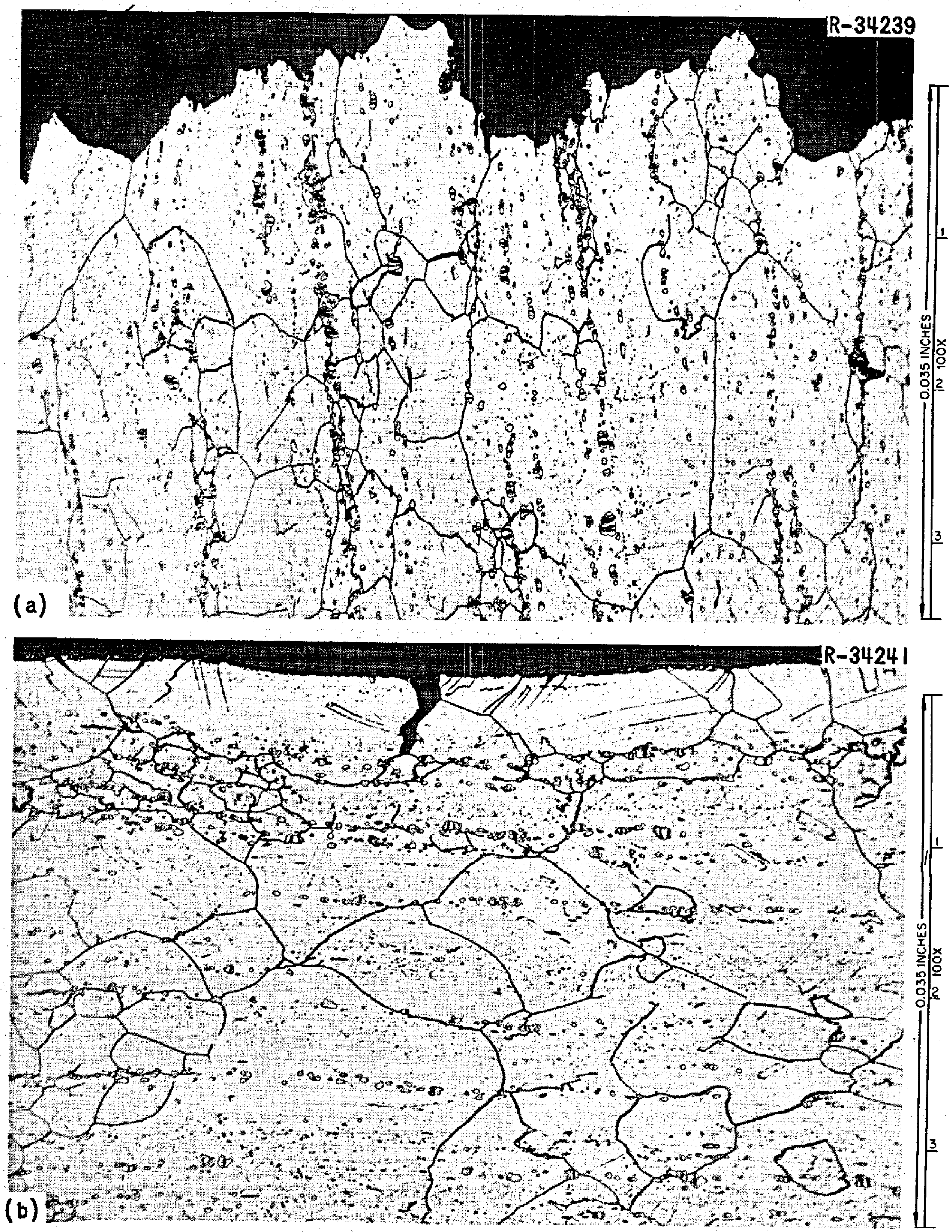

Fig. 29. Photomicrographs of Surveillance Specimen A-16 from Heat 5085 Tested at 25°C and at a Strain Rate of 0.05 min^{-1}. (a) Fracture. (b) Edge of specimen about 1/4 in. from fracture. Etchant: glyceria regia.

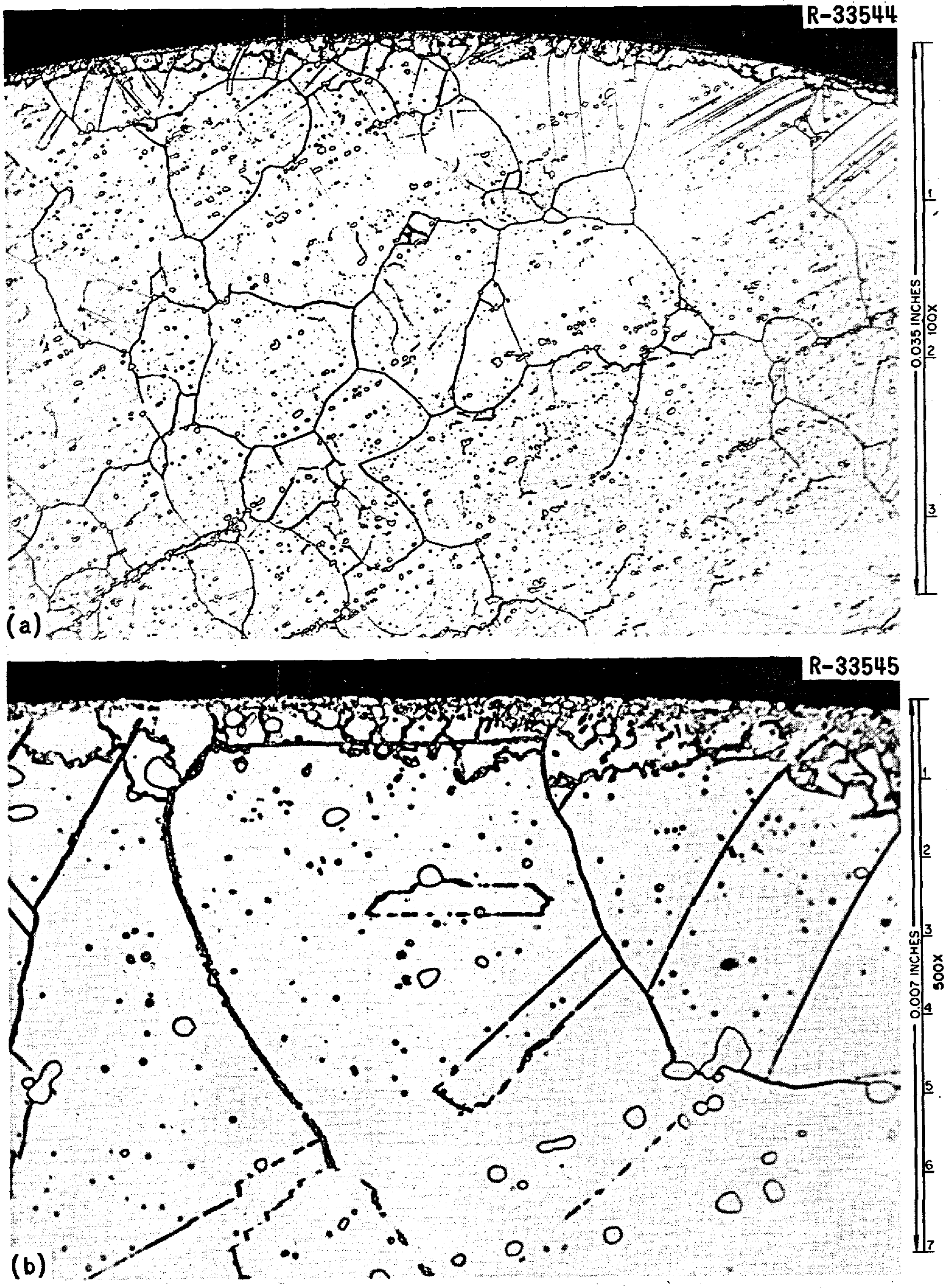

Fig. 30. Cross Section of the Buttonhead of Surveillance Specimen A-16 from Heat 5085 Tested at 25°C. (a) 100 x. (b) 500 x.

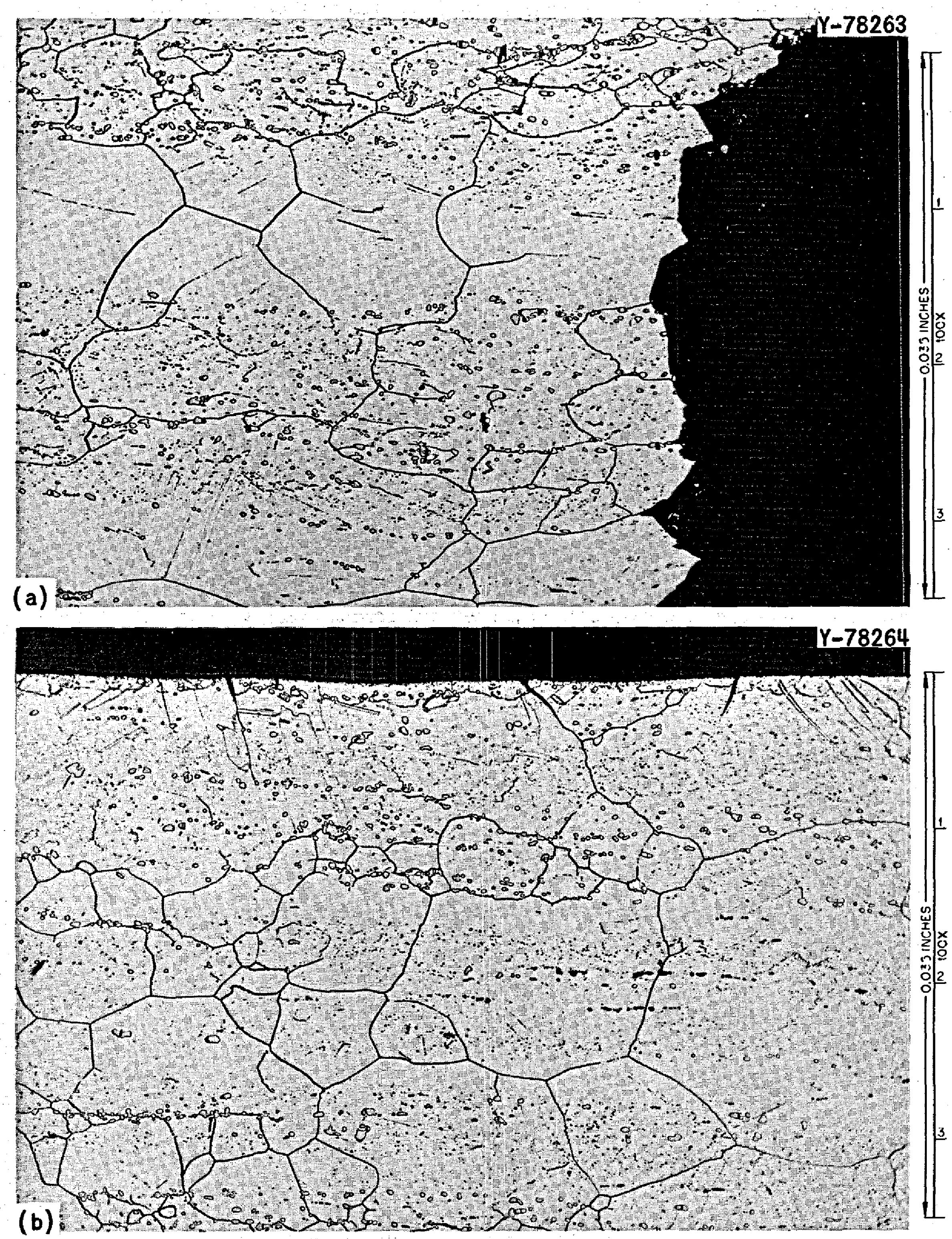

Fig. 31. Photomicrographs of Control Specimen DC-25 from Heat 5085 Tested at 650°C and at a Strain Rate of 0.002 min^{-1}. (a) Fracture. (b) Edge of specimen about 1/4 in. from fracture. Etchant: glyceria regia.

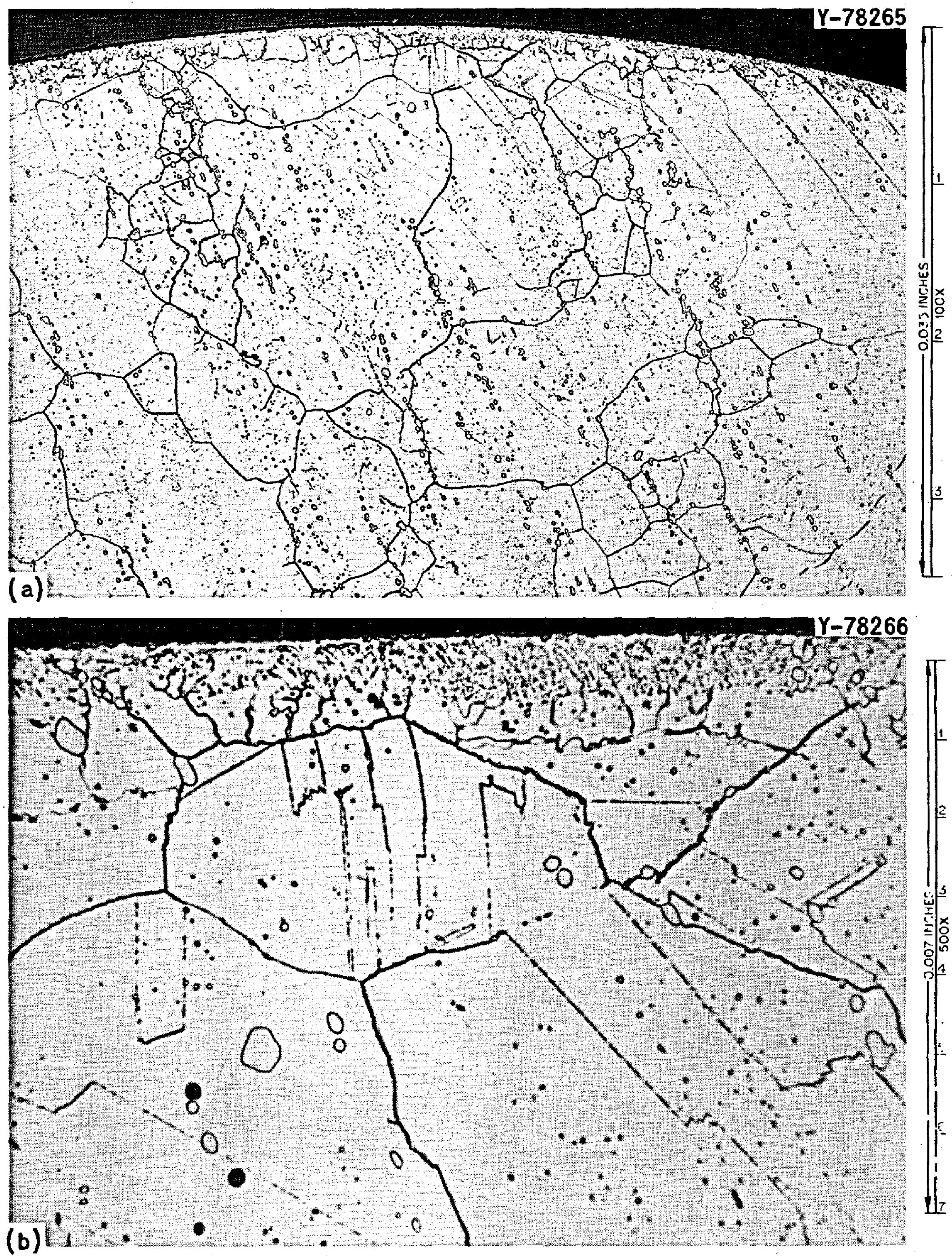

Fig. 32. Photomicrographs of the Cross Section of the Buttonhead of Specimen DC-25. (a) 100 ×. (b) 500 ×. Etchant: glyceria regia.

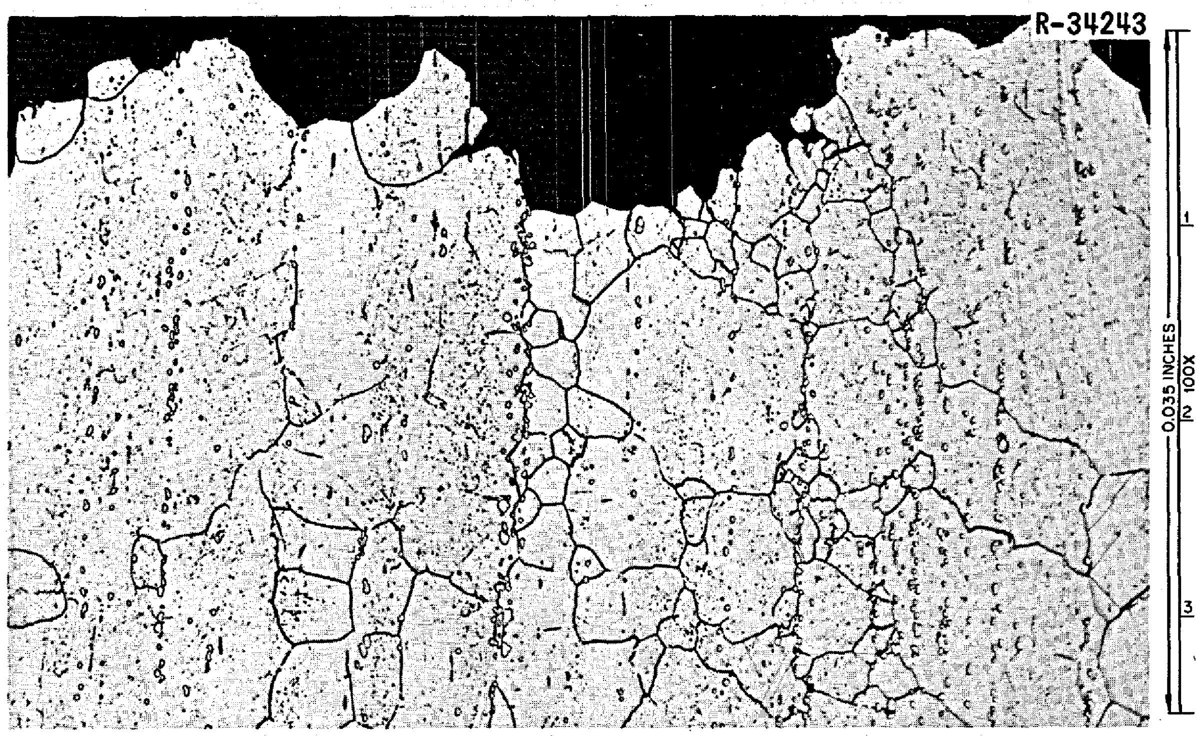

Fig. 33. Fracture of Surveillance Specimen B-6 from Heat 5085 Tested at 650°C and at a Strain Rate of 0.002 min^{-1}. Etchant: glyceria regia.

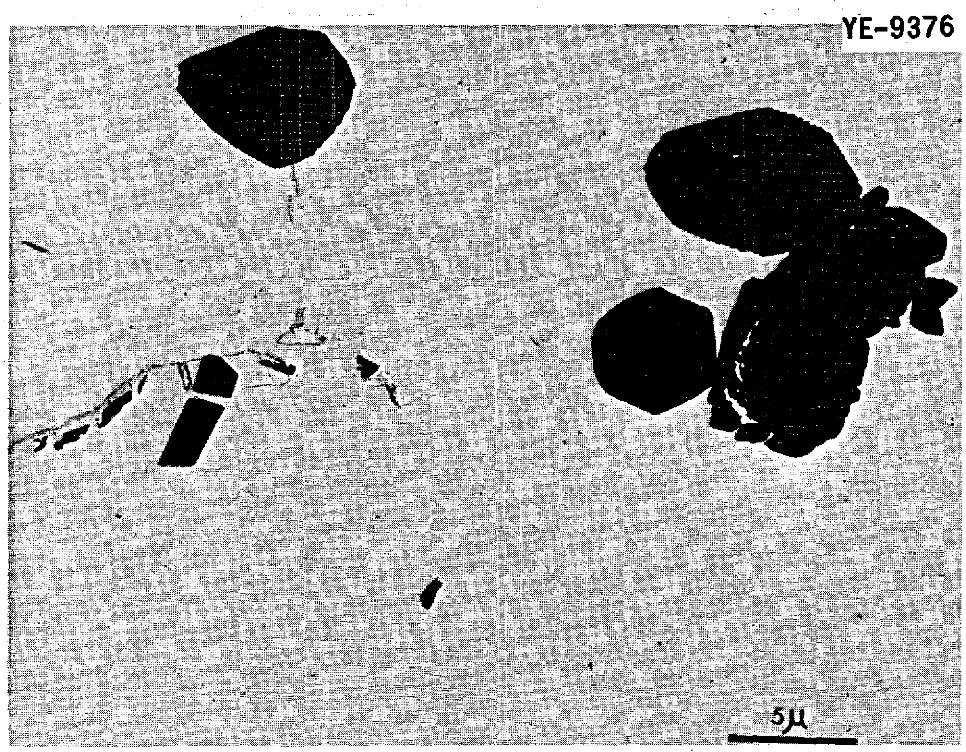

Fig. 34. Extraction Replica from Control Specimen, Heat 5081.

as M_6C. A replica is shown in Fig. 35 for a surveillance specimen from heat 5081. The large M_6C particles are present, but there is a lot of fine intergranular precipitate that has also been identified as M_6C. The irradiation appears to enhance the formation of the fine intergranular precipitate.

Fig. 35. Extraction Replica From Surveillance Specimen, Heat 5081.

DISCUSSION OF RESULTS

Because of the large amount of data presented, we will briefly recapitulate the most important observations.

1. The control specimens from both heats of Hastelloy N exhibited the characteristic ductility minimum in the temperature range of 600 to 700°C. The ductility at various temperatures was reasonably insensitive to strain rate except near 650°C where the ductility decreased with decreasing strain rate.

2. After irradiation the tensile ductility was reduced significantly. There was an unexpected reduction in the room temperature ductility with fracture strains in the range of 35 to 40% being observed. Intergranular fractures were obtained at room temperature in heat 5085. The fracture strain generally became lower as the test temperature was increased and the strain rate decreased.

3. At elevated temperatures (400–850°C) the fracture strains were equivalent for the two heats of surveillance specimens and were found to be the same as those observed previously in other experiments where molten salt was not present.

4. Creep-rupture tests run on unirradiated specimens indicated that the pretest anneal of 2 hr at 900°C improved the rupture strength and ductility over that of the material in the as-received condition. Thus, the stress-relieving anneals at 871°C used in fabricating the MSRE improved the base properties. However, the long exposure of the control specimens at 650°C (operating temperature of the MSRE) caused slight reductions in rupture strength and ductility.

5. The creep-rupture life of the surveillance specimens was less than that of the control specimens, the effect being greater at the higher stress levels. Heat 5085 was affected much as we had observed previously in other experiments on this same heat and other MSRE heats. Heat 5081 exhibited a significant but smaller effect.

6. The creep-rupture ductility of irradiated Hastelloy N goes through a minimum value for a rupture life of from 1 to 10 hr. The fracture strain increases as the rupture life increases (or the stress level decreases). Heat 5081 exhibited appreciably higher fracture strains

than did heat 5085. Heat 5065 (material used for the top and bottom heads of the MSRE) exhibited the lowest ductility of any heat examined to date.

7. A series of tensile tests indicated that prestraining at temperatures over the range of 400 to 850°C did not appreciably lower the fracture strain of the material when tested to failure at 650°C.

8. Neither the control nor the surveillance specimens showed any evidence of corrosion. However, there was a surface product from 0.001 to 0.002 in. in depth that formed where the Hastelloy N and graphite were in contact. Microprobe studies indicate that this layer is high in carbon, and hence the reaction product is probably a metal carbide.

9. Extraction replicas indicated that more intergranular precipitate formed in the surveillance specimens than in the controls. Thus, irradiation must enhance the nucleation and growth of the precipitate (identified as M_6C).

The changes in the unirradiated properties of these heats of Hastelloy N have been demonstrated previously.[7] However, these changes are relatively small, and the properties do not appear to be deteriorating enough for concern. They are probably due to the solution and reprecipitation of M_6C.

The effects of irradiation on Hastelloy N are drastic, but pretty much as expected. Previous work had shown a reduction in the rupture ductility in postirradiation tensile and creep-rupture tests at elevated temperatures.[8,9] These effects are attributed to the helium produced by the $^{10}B(n,\alpha)$ transmutation. Many of the details of the role of helium in metals have been reviewed by Harries,[10] and we have applied these

---

[7] H. E. McCoy, Influence of Several Metallurgical Variables on the Tensile Properties of Hastelloy N, ORNL-3661 (August 1964).

[8] W. R. Martin and J. R. Weir, "Effect of Elevated Temperature Irradiation on the Strength and Ductility of the Nickel-Base Alloy, Hastelloy N," Nucl. Appl. **1**(2), 160–67 (1965).

[9] W. R. Martin and J. R. Weir, "Postirradiation Creep and Stress-Rupture of Hastelloy N," Nucl. Appl. **3**(3), 167 (1967).

[10] D. R. Harries, "Neutron Irradiation Embrittlement of Austenitic Stainless Steels and Nickel-Base Alloys," J. Brit. Nucl. Energy Soc. **5**, 74 (1966).

ideas to Hastelloy N in two recent papers.[11,12] Hence, we shall not discuss the mechanism whereby helium alters the properties. There are some questions concerning the comparison of thermal flux measurements for the MSRE and ORR. However, about 30 to 40% of the ^{10}B was transmuted in the surveillance specimens with a resulting atomic fraction of helium of about 1×10^{-5}. We feel that, at least at low strain rates, the deterioration of properties saturates at helium levels an order of magnitude lower. Hence, the exact helium level is rather academic, and the high-temperature properties have probably stabilized unless continued exposure at 650°C causes metallurgical changes that are detrimental. The drop in ductility at low temperatures is somewhat surprising and bears watching. However, the ductility levels are still quite reasonable.

The mechanical properties appear unaffected by the salt. This is evidenced by the excellent agreement between the results of tests on materials irradiated in the MSRE and the ORR (helium environment). The small amount of carburization that occurred in the Hastelloy N which was in contact with graphite was not surprising and did not extend to alarming depths.

The very low stress levels in the MSRE during normal operation,[13] coupled with the experimental observation that the deterioration of the creep-rupture properties (rupture life and ductility) due to irradiation becomes smaller at low stresses, indicate that transient conditions offer the greatest risk of failure. Thus, with reasonable care in operation, it does not appear at this time that the life of the MSRE will be limited by radiation damage to the Hastelloy N.

---

[11] H. E. McCoy, Jr., and J. R. Weir, Jr., In- and Ex-Reactor Stress-Rupture Properties of Hastelloy N Tubing, ORNL-TM-1906 (September 1967).

[12] H. E. McCoy, Jr., and J. R. Weir, Jr., Effects of Irradiation on the Mechanical Properties of Two Vacuum-Melted Heats of Hastelloy N, (to be published).

[13] R. B. Briggs, private communication.

SUMMARY AND CONCLUSIONS

We have tested the first group of surveillance specimens from the MSRE core. They were removed after 7800 Mwhr of operation during which the specimens were held at 645 ± 10°C for 4800 hr and accumulated a thermal dose of 1.3×10^{20} neutrons/cm^2. Specimens were exposed to molten salt to duplicate the thermal history of the surveillance specimens. Two heats of material, 5081 and 5085, were used with both showing similar deterioration of tensile ductility at elevated temperatures. However, heat 5085 (cylindrical core vessel) exhibited a greater loss of creep-rupture strength and ductility. The property changes were quite similar to those that had been observed for these same materials after irradiation in the ORR where the environment was helium. There was a significant reduction in the low-temperature ductility, but fracture strains of 35 to 40% were still obtained. This change in properties is probably due to the formation of intergranular M_6C.

We noted the formation of a carbon-rich layer on the Hastelloy N where it was in contact with graphite. This layer was only 1 to 2 mils deep and probably would have little effect on the mechanical properties of thick sections. Sacrificial metal shims were placed in the MSRE where the graphite and Hastelloy N were in contact, so the noted carburization should present no problems in the MSRE.

The mechanical properties of the Hastelloy N appear to be quite adequate for the normal operating conditions of the MSRE. However, transients should be prevented that expose the material to high stresses or strains.

ACKNOWLEDGMENTS

The author is indebted to numerous persons for assistance in this study.

W. H. Cook and A. Taboada — Design of surveillance assembly and insertion of specimens.

W. H. Cook and H. B. Piper — Flux measurements.

J. R. Weir, Jr., and W. H. Cook — Review of manuscript.

R. E. Gehlbach — Prepared the extraction replicas.

E. J. Lawrence and J. L. Griffith — Assembled surveillance and control specimens in fixture.

P. Haubenreich and MSRE Operation Staff — Exercised extreme care in inserting and removing the surveillance specimens.

E. M. King and Hot Cell Operation Staff — Developed techniques for cutting long rods into individual specimens, determined specimen straightness, and offered assistance in running creep and tensile tests.

B. C. Willams, B. McNabb, N. O. Pleasant — Ran tensile and creep tests on surveillance and control specimens.

E. M. Thomas, V. G. Lane, and J. Feltner — Processed test data.

H. R. Tinch and E. Lee — Metallography on control and surveillance specimens.

Metals and Ceramics Reports Office — Preparation of manuscript.

Graphic Arts — Preparation of drawings.

INTERNAL DISTRIBUTION

1–2. Central Research Library
3–4. ORNL — Y-12 Technical Library
Document Reference Section
5–14. Laboratory Records Department
15. Laboratory Records, ORNL R.C.
16. ORNL Patent Office
17. R. K. Adams
18. G. M. Adamson, Jr.
19. R. G. Affel
20. L. G. Alexander
21. R. F. Apple
22. C. F. Baes
23. J. M. Baker
24. S. J. Ball
25. W. P. Barthold
26. H. F. Bariman
27. S. E. Beall
28. M. Bender
29. E. S. Bettis
30. F. F. Blankenship
31. R. E. Blanco
32. J. O. Blomeke
33. E. E. Bloom
34. R. Blumberg
35. E. G. Bohlmann
36. C. J. Borkowski
37. G. E. Boyd
38. J. Braunstein
39. M. A. Bredig
40. R. B. Briggs
41. H. R. Bronstein
42. G. D. Brunton
43. D. A. Canonico
44. S. Cantor
45. W. L. Carter
46. G. I. Cathers
47. J. M. Chandler
48. E. L. Compere
49. W. H. Cook
50. L. T. Corbin
51. J. L. Crowley
52. F. L. Culler
53. J. E. Cunningham
54. J. M. Dale
55. D. G. Davis
56. J. H. DeVan
57. S. J. Ditto
58. A. S. Dworkin
59. J. R. Engel
60. E. P. Epler
61. D. E. Ferguson
62. L. M. Ferris
63. A. P. Fraas
64. H. A. Friedman
65. J. H Frye, Jr.
66. C. H. Gabbard
67. R. B. Gallaher
68. H. E. Goeller
69. W. R. Grimes
70. A. G. Grindell
71. R. H. Guyman
72. B. A. Hannaford
73. P. H. Harley
74. D. G. Harman
75. W. O. Harms
76. C. S. Harrill
77. P. N. Haubenreich
78. F. A. Heddleson
79. P. G. Herndon
80. J. R. Hightower
81–83. M. R. Hill
84. H. W. Hoffman
85. R. W. Horton
86. T. L. Hudson
87. H. Inouye
88. W. H. Jordan
89. P. R. Kasten
90. R. J. Kedl
91. M. T. Kelley
92. M. J. Kelly
93. C. R. Kennedy
94. T. W. Kerlin
95. H. T. Kerr
96. S. S. Kirslis
97. A. I. Krakoviak
98. J. W. Krewson
99. C. E. Lamb
100. J. A. Lane
101. R. B. Lindauer
102. A. P. Litman
103. E. L. Long, Jr.
104. M. I. Lundin

105. R. N. Lyon
106. H. G. MacPherson
107. R. E. MacPherson
108. C. D. Martin
109. C. E. Mathews
110. C. L. Matthews
111. R. W. McClung
112–116. H. E. McCoy, Jr.
117. H. F. McDuffie
118. C. K. McGlothlan
119. C. J. McHargue
120. L. E. McNeese
121. A. S. Meyer
122. R. L. Moore
123. J. P. Nichols
124. E. L. Nicholson
125. L. C. Oakes
126. P. Patriarca
127. A. M. Perry
128. H. B. Piper
129. B. E. Prince
130. J. L. Redford
131. M. Richardson
132. R. C. Robinson
133. H. C. Roller
134–138. M. W. Rosenthal
139. H. C. Savage
140. W. F. Schaffer
141. C. E. Schilling
142. Dunlap Scott
143. H. E. Seagren
144. C. E. Sessions
145. J. H. Shaffer
146. G. M. Slaughter
147. A. N. Smith
148. F. J. Smith
149. G. P. Smith
150. O. L. Smith
151. P. G. Smith
152. W. F. Spencer
153. I. Spiewak
154. R. C. Steffy
155. H. H. Stone
156. J. R. Tallackson
157. E. H. Taylor
158. R. E. Thoma
159. J. S. Watson
160. C. F. Weaver
161. B. H. Webster
162. A. M. Weinberg
163. J. R. Weir, Jr.
164. W. J. Werner
165. K. W. West
166. M. E. Whatley
167. J. C. White
168. L. V. Wilson
169. G. Young
170. H. C. Young

EXTERNAL DISTRIBUTION

171. G. G. Allaria, Atomics International
172. J. G. Asquith, Atomics International
173. D. F. Cope, RDT, SSR, AEC, Oak Ridge National Laboratory
174. H. M. Dieckamp, Atomics International
175. A. Giambusso, AEC, Washington
176. J. L. Gregg, Bard Hall, Cornell University
177. F. D. Haines, AEC, Washington
178. C. E. Johnson, AEC, Washington
179. W. L. Kitterman, AEC, Washington
180. W. J. Larkin, AEC, Oak Ridge Operations
181–182. T. W. McIntosh, AEC, Washington
183. A. B. Martin, Atomics International
184. D. G. Mason, Atomics International
185. G. W. Meyers, Atomics International
186. D. E. Reardon, AEC, Canoga Park Area Office
187. R. M. Roth, AEC, Oak Ridge Operations

188. M. Shaw, AEC, Washington
189. J. M. Simmons, AEC, Washington
190. W. L. Smalley, AEC, Washington
191. S. R. Stamp, AEC, Canoga Park Area Office
192. D. K. Stevens, AEC, Washington
193. R. F. Sweek, AEC, Washington
194. A. Taboada, AEC, Washington
195. R. F. Wilson, Atomics International
196. Laboratory and University Division, AEC, Oak Ridge Operations
197–211. Division Technical Information Extension